NASA-CR-192075

NASW-4435

141680

(NASA-CR-192075) TBD(EXP 3) (California Polytechnic State Univ.) 100 p

N93-18054

Unclas

G3/05 0141680

TBD^3

by

Jim Baughan

David Calta

Victor Cross

Mozhi Habashi

Donovan Mathias

Patti Northrup

AERO 443, 444, 445

California Polytechnic State University

San Luis Obispo

Spring 1992

TABLE OF CONTENTS

TABLE OF CONTENTS

LIST OF FIGURES

FIGURES **PAGE NUMBER**

LIST OF TABLES

TABLES		PAGE NUMBER
25	Control surfaces	72
26	Stability derivatives	73
27	Dynamic stability derivatives	74
28	Ticket prices	83
29	Cost analysis of TBD^3	84

LIST OF SYMBOLS

SYMBOLS	DEFINITION
O_3	Ozone
O_2	Diatomic oxygen
hv	Photon energy
NO	Nitrogen oxide
H	Hydrogen
NO_x	Nitrogen oxide compound
HNO_3	Nitric acid
Cl_2	Diatomic chlorine
EPNdB	Effective perceived noise decibels
V_{stall}	Stall speed
L.E.	Leading Edge
V-n	Velocity-g loading
E	Modulus of elasticity
I	Second moment of area
Cl	Lift coefficient
t/c	Thickness ratio
Cl_o	Lift coefficient at zero angle of attack
Cl_{max}	Maximum lift coefficient
T/O	Take-off
L/D	Lift over drag
$C_{D_{wave}}$	Wave drag coefficient
S	Area

SYMBOLS	DEFINITION
b	span
DOC	Direct operating cost
IOC	Indirect operating cost
RTD&E	Research, testing, development, and engineering
$C_{y\beta}$	Variation of side force with sideslip
$C_{y\delta R}$	Variation of side force with rudder angle
$C_{y\delta A}$	Variation of side force angle with aileron angle
C_{yr}	Variation of side force with yaw rate
C_{yp}	Variation of side force with roll rate
$C_{n\beta}$	Variation of yawing moment with roll rate
$C_{n\delta r}$	Variation of yawing moment with rudder angle
C_{nr}	Variation of yawing moment with yaw rate
$C_{l\beta}$	Variation of rolling moment with sideslip angle
$C_{l\delta r}$	Variation of rolling moment with rudder angle
$C_{L\delta e}$	Variation of lift coefficient with elevator angle

SYMBOLS	DEFINITION
C_{lu}	Variation of lift coefficient with speed
C_{lp}	Variation of rolling moment with roll rate
C_{Lq}	Variation of lift coefficient with pitch rate
C_{lr}	Variation of rolling moment with yaw rate
$C_{L\alpha}$	Airplane lift curve slope
$C_{m\alpha}$	Variation of pitching moment with angle of attack
$C_{m\delta e}$	Variation of pitching moment with elevator angle
C_{mu}	Variation of pitching moment with speed
C_{mq}	Variation of pitching moment with pitch rate
C_{mtu}	Variation of thrust pitching moment with speed
$C_{mt\alpha}$	Variation of thrust pitching moment with angle of attack
C_{du}	Variation of drag coefficient with speed
C_{txu}	Variation of X-thrust with speed
$C_{d\delta e}$	Variation of drag coefficient with elevator angle

1.0 INTRODUCTION

A high speed civil transport -- if Orville and Wilbur Wright were a part of the 1991-1992 Cal Poly, San Luis Obispo Senior Design Team, they probably would have thought the task unbelievably difficult and quite possibly a problem that could not be solved; but they definitely would have made an attempt! A similar feeling consumed the designers of the second generation high speed civil transport. When asked by the Aeronautical Engineering staff to design a viable supersonic commercial transport, most of the students were well aware that Boeing, McDonnell Douglas, and other aircraft companies had been studying a cadre of transports for more than 30 years and had yet to present a viable aircraft. In the spirit of aviation progress and with much creative license, the TBD design team spearheaded the problem with the full intention of presenting a marketable high speed civil transport in spring of 1992. The project commenced with various studies of future market demands. With the market expansion of American business overseas, the airline industry projects a boom of over 200 million passengers by the year 2000. This will create a much higher demand for time efficient and cost effective inter-continental travel; this is the challenge of the high speed civil transport.

The TBD^3, a 269 passenger, long-range civil transport was designed to cruise at Mach 3.0 utilizing technology predicted to be available in 2005. Unlike other contemporary commercial airplane designs, the TBD^3 incorporates a variable geometry wing for optimum performance. This design characteristic enabled the TBD^3 to be efficient in both subsonic and supersonic flight. The TBD^3 was designed to be economically viable for commercial airline purchase, be comfortable for passengers, meet FAR Part 25, and the current FAR 36 Stage III

noise requirements. The TBD^3 was designed to exhibit a long service life, maximize safety, ease of maintenance, as well as be fully compatible with all current high-traffic density airport facilities.

Several interior concerns were addressed in the design. The TBD^3 was equipped to accommodate the many needs of our passenger: first class, business, economy (coach). Specific market studies were analyzed so as to best fit our class breakdown to the projected market needs. In addition to interior concerns, external challenges were also addressed. The materials chosen for the TBD^3 allowed minimum weight penalties while maintaining the safety of high-speed flight. The most sensitive weight component was the swing wing mechanism and wing box which spans the fuselage. The structural design and materials were carefully analyzed to minimize the penalty for the swing wing option. With an aircraft this large, (considering specifically thrust power and weight) control surfaces would contribute heavily into the actual feasibility of the TBD^3.

To achieve a neutrally stable aircraft during subsonic and supersonic cruise, fuel pumping and careful fuel placement were utilized. This allowed the aircraft center of gravity to be advantageously manipulated. The aileron and rudder size and placement were designed by integrating all of the stability derivatives for longitudinal, lateral and dynamic stability.

The systems of the TBD^3 were designed to be as conventional as possible. Using standard hydraulic systems with the exception of a digital fly-by-wire control system, the TBD^3 was designed to be serviced and maintained as easily

as any contemporary commercial airplane. TBD^3 engines were selected to be ozone "friendly" at the altitudes of operation.

Finally, the cost analysis allowed the purchaser of the TBD^3 to grasp a projection of research, development and manufacturing costs, as well as economic basis for revenue and profit of the TBD^3. With the technology advances predicted by the designers of the TBD^3, a viable high speed civil transport may be tomorrow's long-range Inter-continental airplane as the 747-400 is today.

2.0 MISSION DESCRIPTION

The mission requirements of the TBD[3] are shown in Table 1.

Table 1 Mission Requirements

Range	4800 nm
Cruise speed	Mach 3.0
Altitude	60,000 ft
Take-off distance	<11,000 ft
Landing distance	<11,000 ft
Take off weight	780,000 lbs
Passengers	269 46% Economy (coach) - 124 39% Business - 105 15% First Class - 40
Crew	1 pilot 1 first officer 7 flight attendants

The range of 4800 nm did not include the international standards for reserves. This range would facilitate a Los Angeles to Tokyo non-stop flight. The following city pairs were included in the mission options.

•London - Miami	3900 nm
•London - New York City	3400 nm
•Paris - New York City	3200 nm
•San Francisco - Tokyo	4500 nm
•Honolulu - Sydney	4550 nm
•Honolulu - Hong Kong	4000 nm
Los Angeles - Tokyo	4800 nm

It has been predicted that the North American market will demand 56% of its flights to Asia and Pacific and 44% to Europe. The city pairs were chosen a result of this market trend and central business centers in the world.

The cruise speed and altitude were chosen to meet the Request For Proposal (See Appendix). The take-off and landing distances were designed to current runway lengths at major International airports and include a standard factor of safety. The crew requirements met FAR 25 minimums and provided each class with service and comfort typical of contemporary air transports. Table 2 provides the flight attendants breakdown.

Table 2 Flight Attendants

First class	2 attendants / 40 PAX
Business class	2 attendants / 105 PAX
Economy (coach) class	3 attendants / 124 PAX

The mission profile of TBD[3] is shown in Figure 2.1.

1. Start-up
2. Taxi
3. Take-off / Climb
4. Acceleration to cruise
5. Cruise / Climb
6. Hold
7. Descent
8. Fly to alternate / Descent
9. Landing
10. Taxi / Shutdown

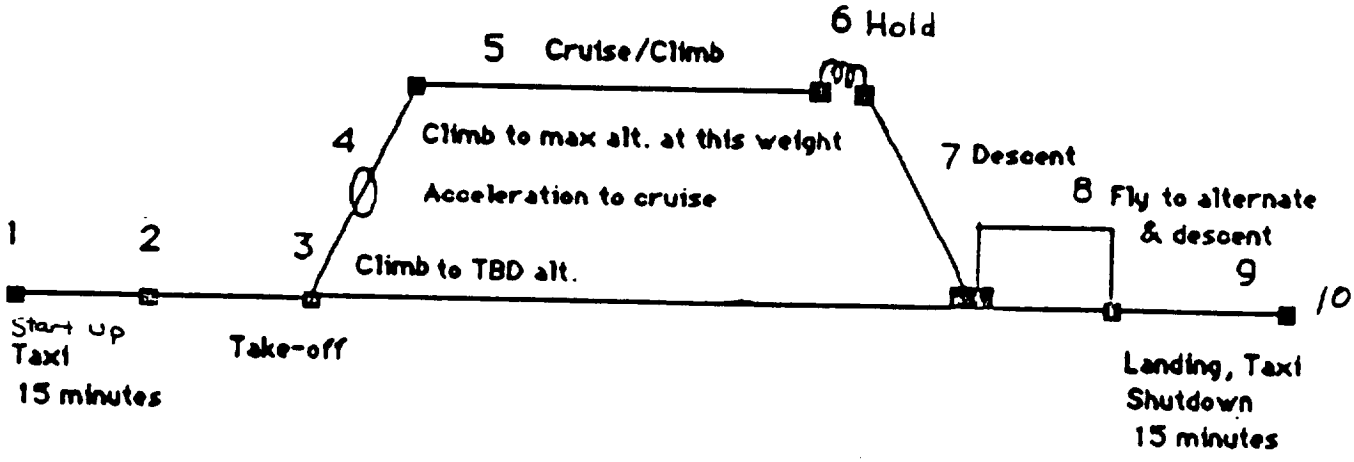

Figure 2.1 Mission Profile Diagram

3.0 ENVIRONMENTAL CONCERNS

3.1 Emissions

A study of stratospheric chemistry was conducted in order to determine the environmental impact of the engine emissions of a fleet of supersonic transport aircraft. No reliable model of the stratospheric chemistry was found and no legislation has been written to describe engine emission parameters. It was found, however, that acceptable emissions and acceptable emission levels must be based against their capacity to destroy ozone. Ozone (O_3) is a molecule that shields the earth from harmful ultraviolet electromagnetic radiation.

Ozone is produced in the stratosphere when diatomic oxygen (O_2) absorbs energy (hν) and is broken into two monatomic oxygen atoms. These atoms are commonly called odd oxygen. The monatomic atoms then react with diatomic oxygen to form ozone. Both the odd oxygen and the ozone are susceptible to attack by reactive molecules in the stratosphere. The reactants that could be produced by aircraft engines are NO, OH, and H. OH emissions are negligible for non-alcoholic fuels.

Reactive nitrogen compounds (NOX) are a product of combustion in air. NOX play a role in ozone destruction in a number of ways. The most obvious is that NOX adds to the natural stratospheric nitrogen reservoir, thereby increasing the amount of NO that can directly attack ozone. NOX contributes to ozone depletion in two other significant ways (see Appendix), but it acts as a catalyst rather than an attacking reagent.

Current research and development in both government laboratories and in industry is addressing the impact of the above mentioned concerns on future aircraft engine design. TBD[3] was designed to cruise in the stratosphere at 60,000 ft. The engines selected for TBD[3] are currently under development for future high speed civil transports, therefore they are being designed with emission restrictions.

3.2 Community Noise

The maximum allowable community noise levels are specified in the FAR 36 Stage III requirements. There is a possibility of Stage IV requirements in the making but the time parameters involved in implementing Stage IV have not been established. Stage IV would require a 4 EPNdB (Effective Perceived Noise dB) reduction for all flight conditions regulated by Stage III. Current research into supersonic transport power plants indicate that meeting Stage III requirements will be a formidable technical challenge; complying with Stage IV requirements was decided to be an overly stringent design criteria. Stage III regulations are summarized in Table 3.

Table 3 Stage III Regulations

FAR Part 36 Stage III	EPNdB level
Takeoff	106
Sideline	103
Approach / Landing	105

The high lift, low drag capability of the variable sweep wing allowed TBD[3] to take-off at a moderate speed, therefore reducing the take-off and sideline noise produced by the engines. This resulted in the compliance of the engines with FAR 36, Stage III.

Sonic Boom Over pressure

It was found that a 1.2 psf sonic boom over pressure would result in insignificant public annoyance and no structural damage (Reference 15). This over pressure is comparable to distant thunder. The mentioned over pressure value corresponds to a far-field N-wave (rise time of essentially zero). If the rise time is increased, the perceived strength of the shock wave is diminished. If the rise time was greater than or equal to 20ms, a maximum over pressure of 2psf would be acceptable (Reference 16). The rise time reduces the perceived over pressure to about 1.2psf. This moderation of the perceived strength of the shock wave was intended to curb public annoyance only; the actual strength, as far as structures are concerned, was not reduced by increasing rise time.

4.0 INTERIOR CONCERNS

TBD^3's interior was designed to comply with FAR part 25 requirements. This compliance included boarding, service, and emergency doors. Lavatories, galleys, and storage space for the passengers were also included as the interior concerns. Table 4 lists the type and number of doors on TBD^3 and they are illustrated in Figure 4.1.

Table 4 Doors on the TBD^3

Door	Quantity	Type	Dimension	Position
Boarding	2	A	42" x 76"	Front of coach & first class Left side
Service	3	A	42" x 74"	Upper and lower deck Right side
Emergency	2	III	20" x 38"	Lower deck Left and right side
Emergency	1	I	48" x 24"	Upper deck Left side

FOLDOUT FRAME 1

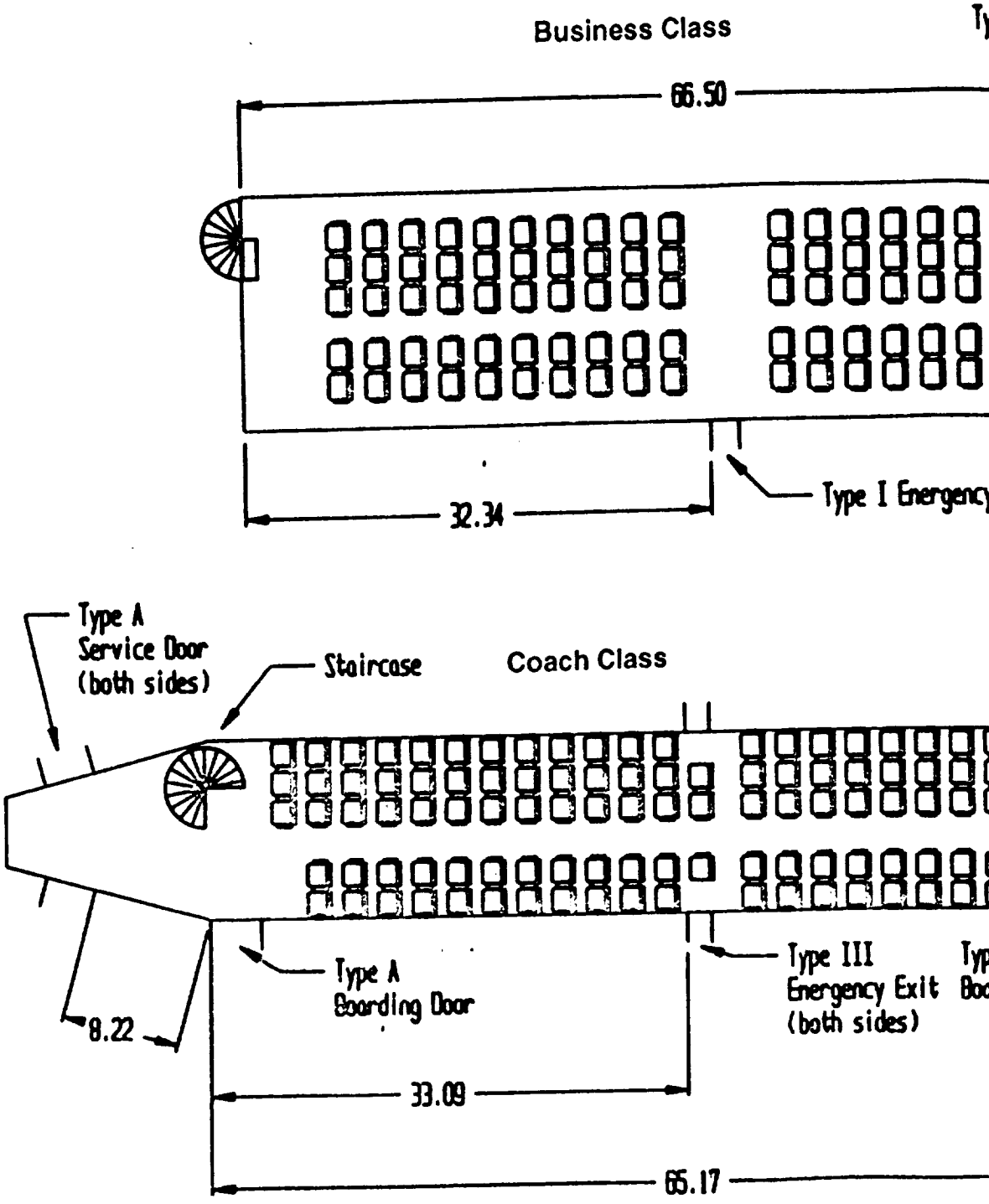

Figure 4.1 Doors on

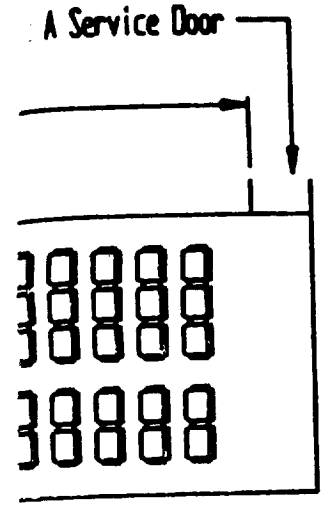
A Service Door

Exit

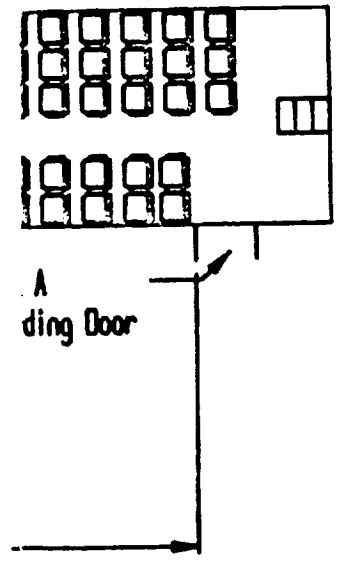
A
ding Door

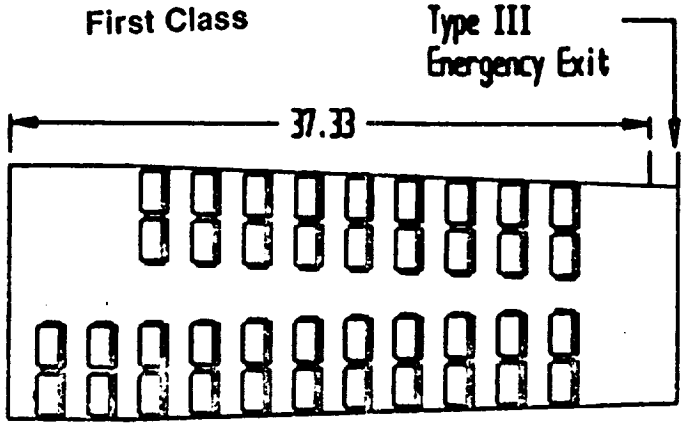
First Class
Type III
Emergency Exit
37.33

BD3

Galleys were specifically designed for each class to accomadate the number of passengers (Table 5). Galley type A cut in half was placed in front of the coach class on both sides of the walls as shown on the Figure 4.2. The floor at this section has been raised approximately 5 inches to accommodate the nose landing gear into the fuselage. Another type A galley was placed in the aft section of the business class on the upper deck of the fuselage, and a type B galley was placed in the first class section (Figure 4.2).

Table 5 Galleys on the TBD[3]

Galley	Location	Maximum Capacity	Dimension
A	Coach Class Business Class	12 tray carriers 8 ovens 229 entrees	79" x 33" x 78"
B	First Class	4 tray carriers 2 ovens 42 entrees	48" x 24" x 78"

FOLDOUT FRAME

Business Class

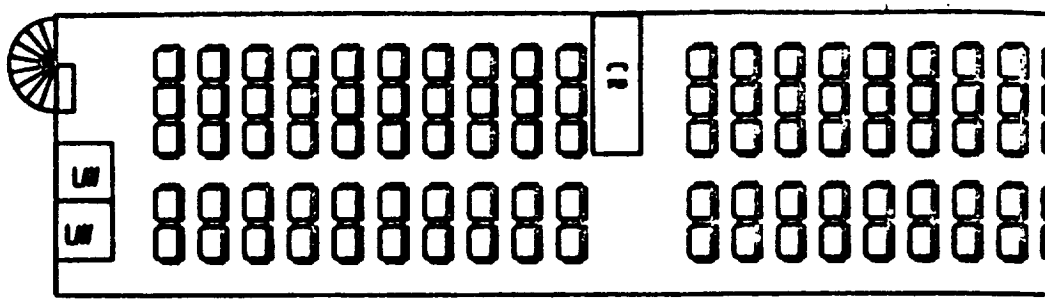

Coach Class

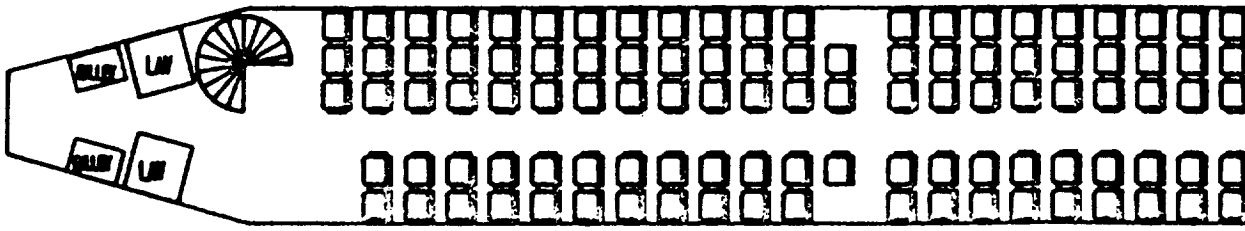

Figure 4.2 Galleys, Lavatories, &

FOLDOUT [illegible] 2.

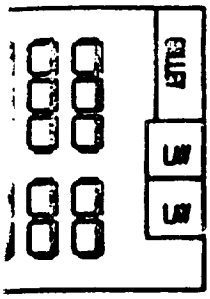

First Class

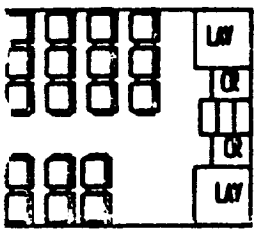

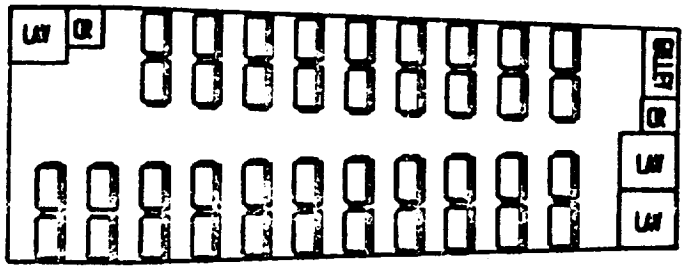

Coat Racks on TBD[3]

Lavatory placement in the fuselage is shown in Figure 4.2. Three lavatories have been placed in first class, four in coach, and four in business class. The lavatories have been designed as 40" x 40" x 78.0". The interior storage was designed in the form of over head carry-on bins in first and coach classes, and side storage bins in business class (Figure 4.3). The over head carry-on bin size was designed to accomodate a folded garment bag, and the side storage bin to accomodate a brief case.

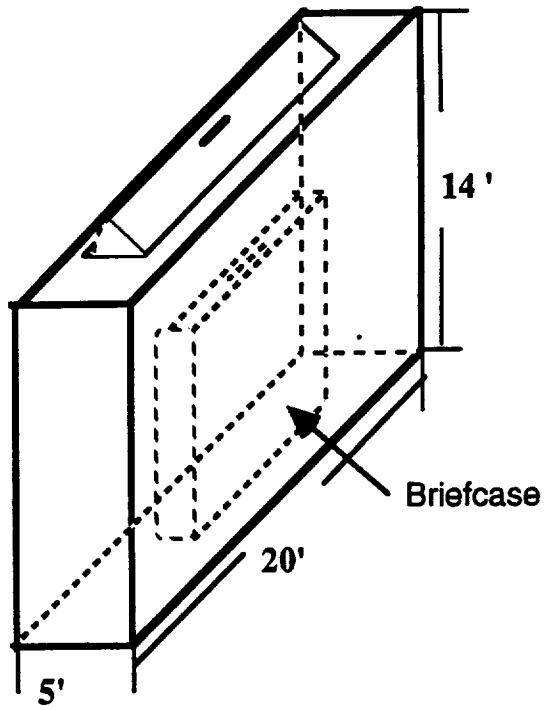

Figure 4.3 Side Storage

5.0 SIZING ANALYSIS

5.1 Thrust and wing loading

Thrust loading versuss wing loading constraint curves were calculated using a computer design program and the method outlined in Reference 1 and the weights in Table 6. The design of the aircraft was based on thrust and wing loading required at take-off, stall speed (Vstall), and available engine thrust. Sizing the TBD^3 to the required thrust and wing loading yielded a design point with a thrust to weight ratio of 0.27 and wing loading of 110 psf. (See Appendix)

5.2 Take-off weight sizing

A preliminary takeoff weight was calculated for the TBD^3 using procedures outlined in Reference 1. This procedure yielded the empty weight and take-off gross weight of the aircraft. The weight fractions used for each mission segment and the total weights are shown in the Table 6.

Table 6 Weight Fractions

Start & Warm-up, W1	W1/Wto	0.99
Taxi, W2	W2/W1	0.995
Take-off, W3	W3/W2	0.995
Climb, W4	W4/W3	0.88
Cruise, W5	W5/W4	0.60
Loiter, W6	W6/W5	0.95
Descent, W7	W7/W6	0.98
Alternate (optional), W8	W8/W7	0.971
Landing, W9	W9/W7	0.99
Empty Weight	We	380,000 lbf
Take-off weight	Wto	780,000 lbf
Final Fuel Fraction	We/Wto	0.48

6.0 CONFIGURATION

6.1 Design Trade Study

A trade study comparing aerodynamic performance of different wing planforms was conducted to determine the basic configuration of TBD^3. After surveying historical and existing aircraft with supersonic cruise capability, delta and variable-geometry wings were chosen to be examined.

The delta wing configuration offered adequate supersonic performance, but at low-subsonic speeds it required a high angle of attack to generate required lift. It was determined that a delta wing configuration would not generate enough lift to take off due to a limited rotation angle. This is illustrated in Figure 6.1 which shows typical delta wing versus TBD^3's wing performance.

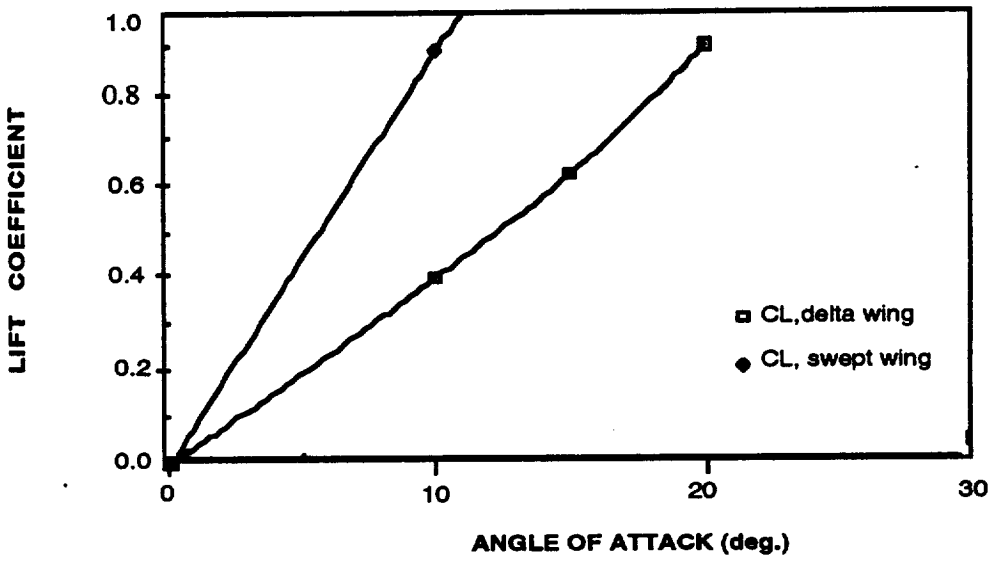

Figure 6.1 Delta Wing Versus Conventional Swept Wing

The variable-geometry configuration offered the necessary supersonic performance without a significant penalty in subsonic performance. The counter point to the aerodynamic advantage is a substantial weight penalty (estimated 18% heavier than a fixed-geometry wing) associated with the structural complexity of a variable-geometry wing.

A trade study comparing different fuselage longitudinal shapes was conducted and the results of the trade study varied widely depending on wing selection. The delta wing configuration allowed for a conventional fuselage shape that tapered in radius due to area ruling. The variable geometry configuration, however, required an unconventional fuselage shape. The variable-geometry wing required a massive structural element (the wing box) as well as a massive hydraulic actuator system Structural integrity required the wing box to traverse the fuselage. This limited passenger mobility and prohibited passenger seating aft of the wing box. To retain the desired number of passengers, double deck seating forward of the wing box was necessary. Thus, a large fuselage diameter forward of the wing box followed by sharp taper aft of the wing box (for area ruling) was required.

Circular versus double-bubble cross sections were then examined. Circular cross sections offered the optimum pressure vessel shape and were less complicated to analyze and to construct compared to the double-bubble. The double-bubble, however, offered a more efficient utilization of cross sectional area for the delta wing configuration.

The issue of whether or not to have passenger windows was addressed. For a civilian transport with a 60,000 ft cruise altitude at Mach 3.0, eliminating

windows had safety and weight savings advantages. The pressure differential at 60,000 ft made any window failure very dangerous to passengers. Weight saved by eliminating windows was two-fold; windows are heavier than skin, and less fuselage frames were necessary because they could be spaced further apart. The disadvantage of not having windows is that it has never been tested on a civilian transport. To alleviate any passenger uneasiness video monitors were to be used to project scenic exterior views.

6.2 Configuration Description.

Because of the aerodynamic advantages of the variable-geometry configuration, the accompanying weight penalty was deemed acceptable, and a variable-geometry configuration was adopted. The mechanism and wing box were designed to be similar to the system used on the B-1 bomber. TBD^3 was designed to take off with the wings swept 12° aft and cruise supersonicly with wings swept 60° aft. These angle limits were due to the swing mechanism's geometric limitations. Double deck passenger seating and cargo storage was positioned forward of the wing box and most systems and fuel were stowed aft of the wing box. A circular cross section offered ample space for double decker seating. Whitcomb's area ruling principle was employed to shape the fuselage aft of the wing box. To approximate a Sears-Hack area distribution, it was found that the fuselage needed to taper considerably in the wing-fairing length. A conventional tail with vertical and horizontal stabilizers was used. Figure 6.2 is a 3-View of the TBD^3

FOLDOUT FRAME 1

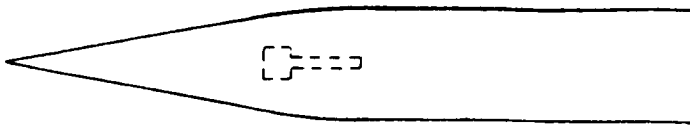

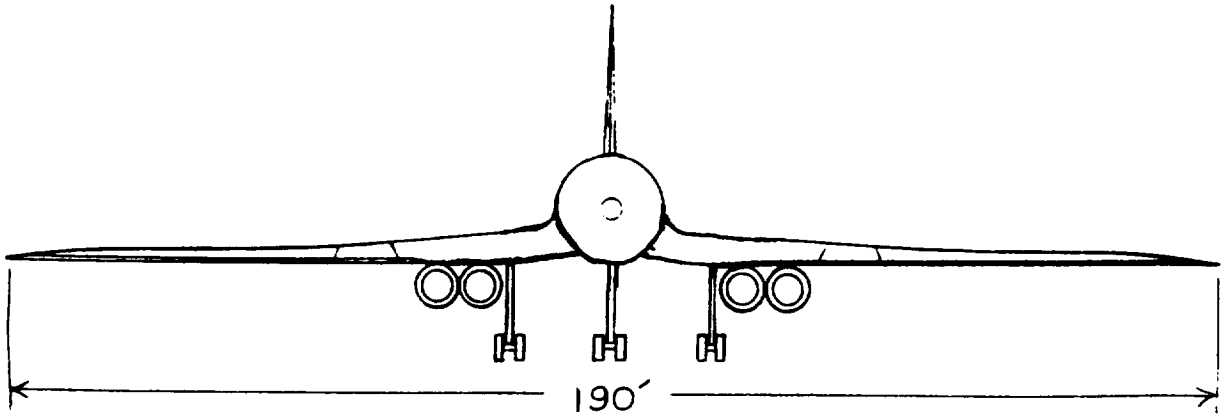

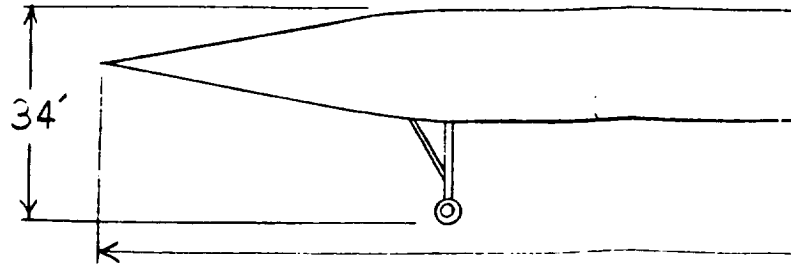

Figu

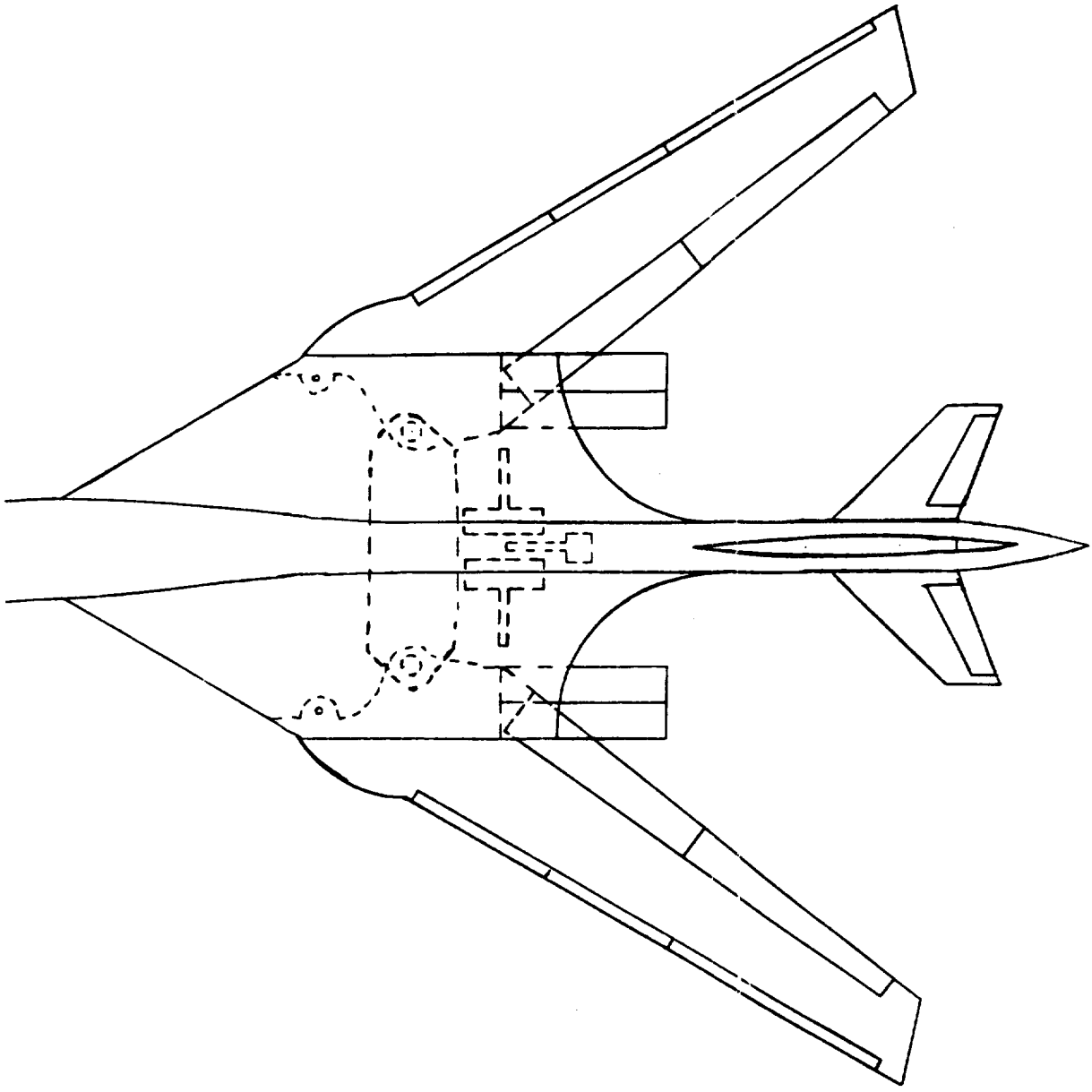

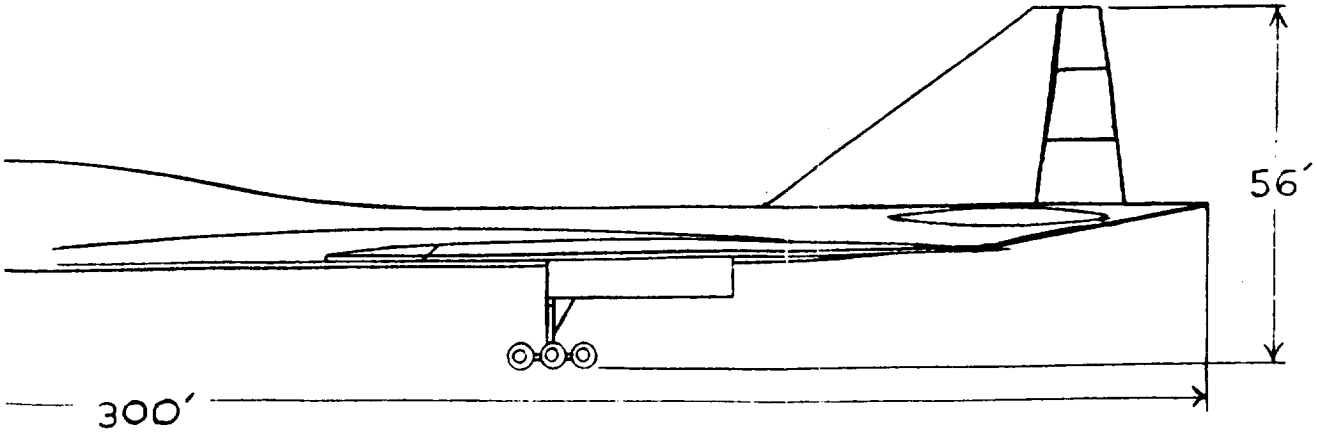

e 6.2 TBD[3] 3-View

7.0 COMPONENT DESIGN

7.1 Wing

A variable geometry wing was chosen for use on TBD^3. This planform offered excellent performance at subsonic and supersonic speeds. The driving force of the design was the need for efficient supersonic cruise. This was the most important factor due to the large portion of the total block time spent at these conditions. A highly swept or delta type wing offered this requirement. Another critical requirement was the ability to generate moderately high lift coefficients (near 1.0) at reasonable angles of attack (less than 12 degrees). This was necessary for the aircraft to take off from contemporary airports. Lower lift coefficients required larger wing areas or higher take off speeds. Larger wings were heavy, expensive, and had high drag at cruise speeds. The extra area provided by the larger wings was not needed at cruise speeds because of the high dynamic pressure. High take-off speeds also increase weight and cost while creating more noise. The variable geometry wing offered solutions to the previously introduced aerodynamic problems. To avoid having to sweep behind the 71° Mach cone, a supersonic airfoil was used. Active leading edge control were used to maintain attached flow subsonicly. The aft swept position was set at 60° (measured from leading edge) to give lowest possible drag conditions while maintaining a realistic mechanism. For take-off, the wing was set at a leading edge sweep angle of twelve degrees again due to pivot restraints. This allowed the development of sufficient lift to take-off at safer speeds while generating less noise. This was thought to be critical for an aircraft to be successful in the future, with the impending possibility of instatement of more stringent noise regulations. An additional advantage of variable geometry

wings was the ability to efficiently cruise at any subsonic speeds. While this was not a primary design goal, it drastically increased the flexibility of the aircraft. Sonic boom restrictions ruled out the possibility of supersonic flight over populated areas, so the ability to subsonic cruise efficiently reduced the penalty of flying over the continents. This offered a distinct advantage over the delta-wing configuration.

Once the variable geometry design was chosen, the other wing parameters were considered. The wing area was fixed by take-off wing loading constraints. From this the largest realistic aspect ratio that would achieve the needed area was employed. This reduced the induced drag as much as possible. Additionally, the taper ratio was chosen to simulate, as closely as could be expected, an elliptic planform to further reduce induced drag (Reference 17) Overall, the variable geometry wing exhibits excellent lift and drag characteristics throughout the entire flight regime. Table 7 contains the wing parameters.

Table 7 Wing Parameters

Planform Area	7000 ft^2
Root Chord	36 ft
Tip Chord	15 ft
Aspect Ratio M<1	10.5
Aspect Ratio M>1	5.6
Airfoil	biconvex 4% thick
Take Off L.E. Sweep	12°
Supersonic Cruise L.E. Sweep	60°

7.2 Empennage

A study of different empennage configurations was conducted to find out which would best suit the needs of the TBD^3. This study consisted of a canard, three-surface, tailless, and conventional empennage configuration.

The canard configuration was found to be theoretically more efficient than an aft-tail because the canard's lift reduced the lift the wing needed to produce. This permitted a smaller wing and reduced total induced drag. Unfortunately, the use of a canard contributes to the aircraft's instability by driving the location of the wing further aft than would be the case with an aft tail. This would increase the pitching moment caused by the use of wing flaps.

Theoretically, on a three-surface configuration, the canard and aft tail can act in opposite directions, thus canceling out each other's effect upon the total lift distribution. The main drawbacks of this configuration, however, were the additional weight, complexity, and interference drag associated with the extra surfaces.

The tailless configuration offered the lowest weight and drag of any configuration. The tailless design was sensitive to the location of the c.g., and was most successful when the expendable fuel and payload were located very close to the center of gravity.

After studying these various configurations, a conventional tail was decided upon for the TBD^3. The reason was that the conventional tail provided adequate stability and control at the lightest weight and with the least amount of

complexity. A conventional low horizontal stabilizer was placed on the fuselage. This positioning located the tail close to the wing wake which increased the induced flow over the horizontal tail (Reference 9). This had to be taken into consideration when sizing the tail. The tail was sized using the volume coefficient method in Refernce 3. Tables 8 and 9 contain the specific geometry of the horizontal and vertical tails.

Table 8 Horizontal Tail Geometry

Area	800 ft^2
Leading Edge Sweep	45°
Root Chord	25 ft
Tip Chord	9 ft
Taper Ratio	0.36
Span	49 ft.
Aspect Ratio	3.0

Table 9 Vertical Tail Geometry

Planform Area	1025 ft^2
Leading Edge Sweep	54°
Root Chord	57 ft
Tip Chord	11 ft
Taper Ratio	0.19
Height	31 ft
Aspect Ratio	.94

7.3 Fuselage

Flying at Mach 3.0 demanded that special attention be paid to Whitcomb's area rule to reduce wave drag. Fuselage shaping and wave drag calculation were interdependent and iterated to the final solution. Section 10.3 provides more details regarding the area distribution and resulting wave drag.

The fuselage was designed to facilitate double deck seating forward of the wing box. Inner diameter was sized to optimize floor widths while retaining a 78 inch ceiling height for both decks (see Figure 7.2). Six inches was allowed for frames, stringers, insulation, and interior lining. The resulting inner radius was held constant from the end of the nose cone to the fairing leading edge. The outer radius of this section increased 6 inches for area ruling purposes. The fuselage then tapered linearly to the fairing-wing trailing edge intersection. This taper was such that the bottom of the fuselage remained flat. The next section had constant radius and continued to within 40 ft of the tail cone. At this point the radius tapered to the tail cone such that the top of the fuselage remained flat. The location of this section of taper was determined by rotation angle necessity.

Table 10 Fuselage Geometry

Nose 1/2 Angle	10°
Distance From Nose (ft)	Fuselage Radius (ft)
44	8.67
124	9.67
218	4.00
260	4.00
300	0.50

7.4 Flight Deck

The flight deck of the TBD[3] resembled those of most contemporary commercial transport jets. The most notable difference, however, will be the absence of windows for the flight crew. Instead, a synthetic vision system will be used. The synthetic vision system was necessary to eliminate a rotating nose configuration. This configuration was used on the Concorde to enhance pilot visibility at high angle of attack. A flight deck layout is shown in Figure 7.1.

Table 11 Flight Deck Contents

A	Flight crew seats
B	Observer seat
C	Common console
D	Single console (2)
E	Radio Rack
F	Electronics
G	Viewing screen

Figure 7.1 Flight Deck Layout
Top View

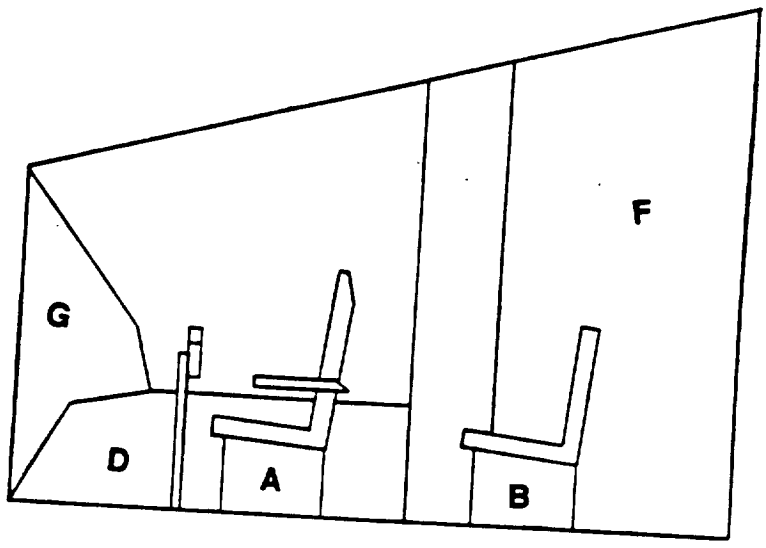

Figure 7.1 Continued
Side View

7.5 Passenger Placement

All passenger seats on TBD^3 were placed forward of the wing box. Space for the coach and business classes was allocated in the double deck section; first class was placed on its own level in the tapering section of the fuselage (Figure 4.2). Business class was placed on the upper deck and coach on the lower. The first class floor is 24 inches higher than that of coach class. The intent was for first class to board first, then the business class would get to the upper deck via a spiral staircase, and finally coach class would board. Since the first class will leave last the flight attendants will provide complimentary drinks and/or snacks while they wait. The boarding doors on TBD^3 have been designed so if the leaving of first class arises a problem, the airline has the option of using the boarding door close to the first class so they can leave as well as board first.

This seating configuration allowed for 124 coach passengers, 105 business passengers, and 40 first class passengers.

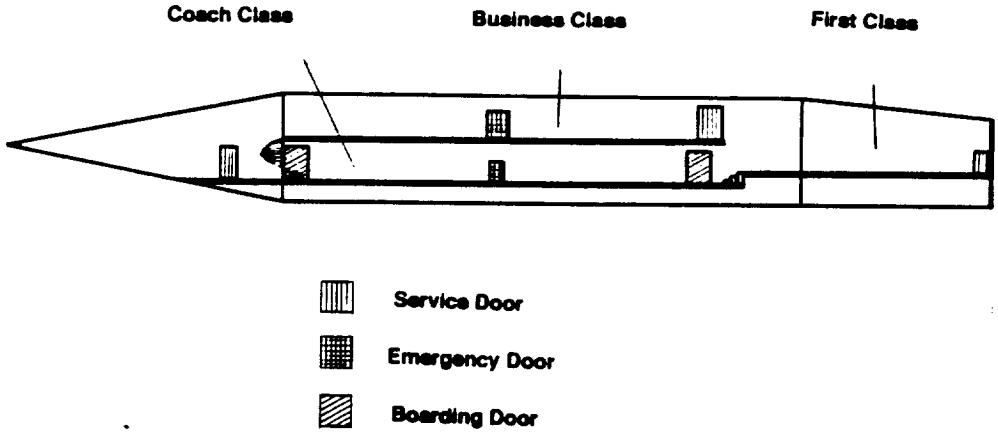

Figure 7.2 Seating Configuration

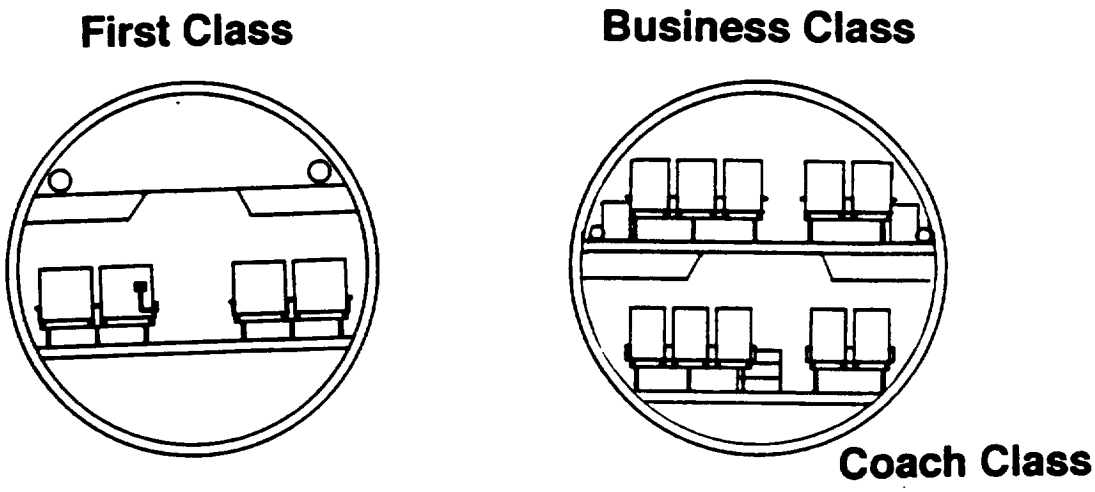

Figure 7.2 Continued Seating Configuration

7.6 Fairing

A large structure was needed to house the wing pivot mechanism, attach engines, and to store fuel. It was decided that a wing fairing would serve these purposes and also provide wing-fuselage blending to reduce interference drag. The size was a trade off between the large size desired for fuel storage and efficient structures design and the long, thin shape representative of low wave drag. The final fairing geometry was as thick as possible while mainting a favorable area distribution (See Appendix).

Table 12 Fairing Geometry

Root Chord	100.00 ft
Tip Chord	50.00 ft
Half Span	330 ft
Average Thickness	4.00 ft
L.E. Sweep Angle	60°

7.7 Propulsion

The engine selection for TBD^3 supersonic transport was based on high performance and low specific fuel consumption during subsonic and supersonic flight. Low engine noise and high thrust production were also an important factor in engine selection.

The engine selected for this aircraft was a General Electric 21/J9B2 Double bypass - dual cycle engine. This is a General Electric study engine which has been tested for Mach 2.4, and 60,000 ft altitude. The GE 21/J9B2 engine was designed to have a bypass ratio of 4.0 at takeoff and 0.52 during supersonic flight. The method presented in Reference 2 chapter 10, was used to estimate the weight, length, and inlet diameter of the engine needed for the TBD^3 supersonic transport (See Appendix). The results calculated were as follows:

Table 13 GE 21/J9B2 Double bypass - Dual cycle Engine Specifications

Installed Thrust	Total weight	Total Length	Inlet diameter
53,000 lbf	12,784 lbf	23.00ft	7.55 ft

Cycle pressure ratio	22.40
Takeoff bypass ratio	4.00
Supersonic bypass ratio	0.52
Specific Fuel Consumption M<1	0.60 lb/lb/hr
Specific Fuel Consumption M>1	1.40 lb/lb/hr

Turbojet/turbofan engines are incapable of efficient operation unless the air entering them is slowed to a speed of about Mach 0.4-0.5. This is to keep the tip speed of the compressor blades below sonic speed relative to the incoming air. Slowing the speed of the incoming air is the primary purpose of an inlet system. The conical inlet used in the TBD^3 engines exploited the shock patterns created by supersonic flow over a cone. This inlet system was designed as a four-shock system which consisted of three oblique shocks to decrease the mach number and one normal shock wave to make the flow subsonic (Figure 7.3). This inlet system provided the TBD^3 engines with a total inviscid pressure recovery of 86%. The inlet was also variable, where the second ramp had a variable angle, and was able to collapse and open a larger duct opening for subsonic flight as shown in Figure 7.4.

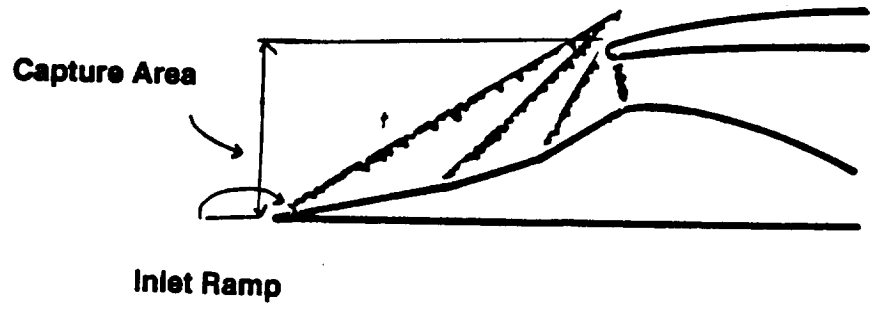

Figure 7.3 4-Shock Inlet System

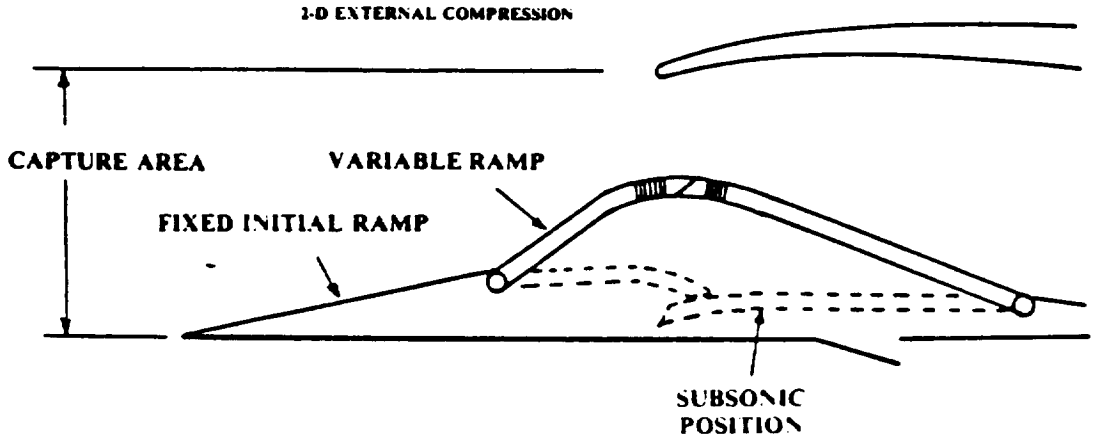

Figure 7.4 Variable Inlet Geometry

The location of the engines on TBD[3] were dependent on factors such as the structure of the aircraft, interference drag. It was undesirable to place the engines on the swinging portion of the wing because of the associated rotation mechanism. Inlet locations were designed to avoid any interference with the main landing gear. The engine nacelles were positioned up at a two degree angle with respect to the wing just forward of the trailing edge. The engine inlet locations provided the aircraft with constructive interference as shown in a study by Douglas Aircraft Company (Reference 13) This interference increased the L/D due to external compression by the inlets.

The connection of the nacelles was designed so that they could be connected to the bottom face of the wing without pylons to decrease skin friction and interference drag (Reference 11). The nacelles were connected to the structure inside the wing as shown in Figure 7.5. This installation provided the aircraft with a weight saving advantage due to no pylons and shorter landing gear. Four separate nacelles were chosen after a priliminary trade study involving the skin friction drag, pressure recovery, inlet drags, and nacelle weights. Based on wave drag of the complete configuration analysis separate nacelles were the favored configuration (Reference 10). The nacelle positions forward or aft of the fuselage greatly affected the wave drag. By placing the nacelles as far aft as structurally permissible the wave drag was reduced.

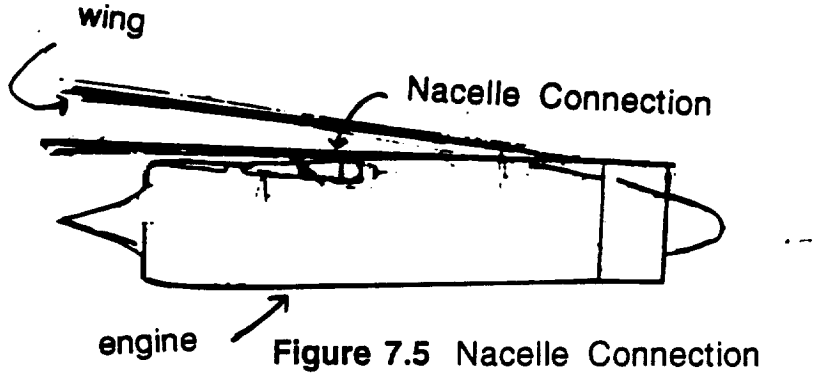

Figure 7.5 Nacelle Connection

Allowable engine noise is governed by FAR 36, Stage III. Contribution to noise included jet mixing noise and shock noise. The noise suppressers used in the engines of TBD[3] were effective by shifting the emitted energy to higher frequency. This fact was one of the contributors to meeting the Stage III requirements (Reference 12).

A converging-diverging ejector nozzle and acoustic lining were used for noise suppression in the TBD[3]. The reduction of noise by the nozzle was achieved by reducing the annulus height, therefore transferring the acoustic energy to a higher frequency. The exit velocity at take-off causes the sideline noise which produces public annoyance. The acoustic lining and the nozzle used in this engine were designed to produce low enough exit velocity to comply with Stage III (See Appendix). Another advantage of the converging-diverging ejector nozzle was that it provided noise reduction throughout power changes (subsonic to supersonic). Engine location on the wings and fuselage also reduced noise. Wings and fuselage of the TBD[3] reflected and scattered sound away from ground based receivers (Reference 12).

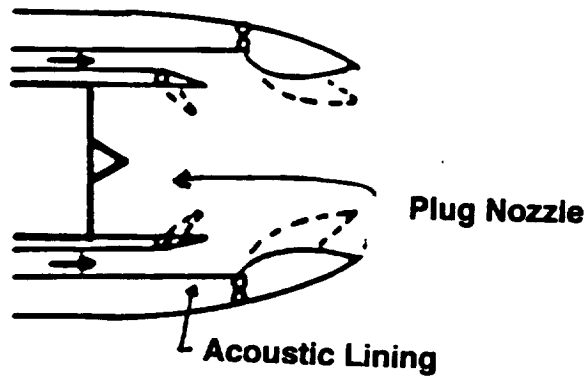

Figure 7.6 Converging-Diverging Ejector Nozzle

7.8 Landing Gear

The first concern regarding landing gear for the TBD^3 was the volume required to store the landing gear when the aircraft was in the cruise configuration. Typical subsonic transport category aircraft rely on large fairings around the wing root to provide the room necessary to store the large tires and hydraulic mechanisms. These fairings were not an option on the TBD^3 due to the large amount of drag produced by any protrusions from the fuselage. This one limitation had a large impact on the decision to proceed with the design selection of TBD^3. The design was deemed capable of storing the necessarily large and numerous tires required. Figure 7.7 shows that the main gear retracts into the fuselage proper in an area that does not contain passengers. This area is located just aft of the main wing box so that the necessary structure of the main landing gear can be connected to the structurally sound member.

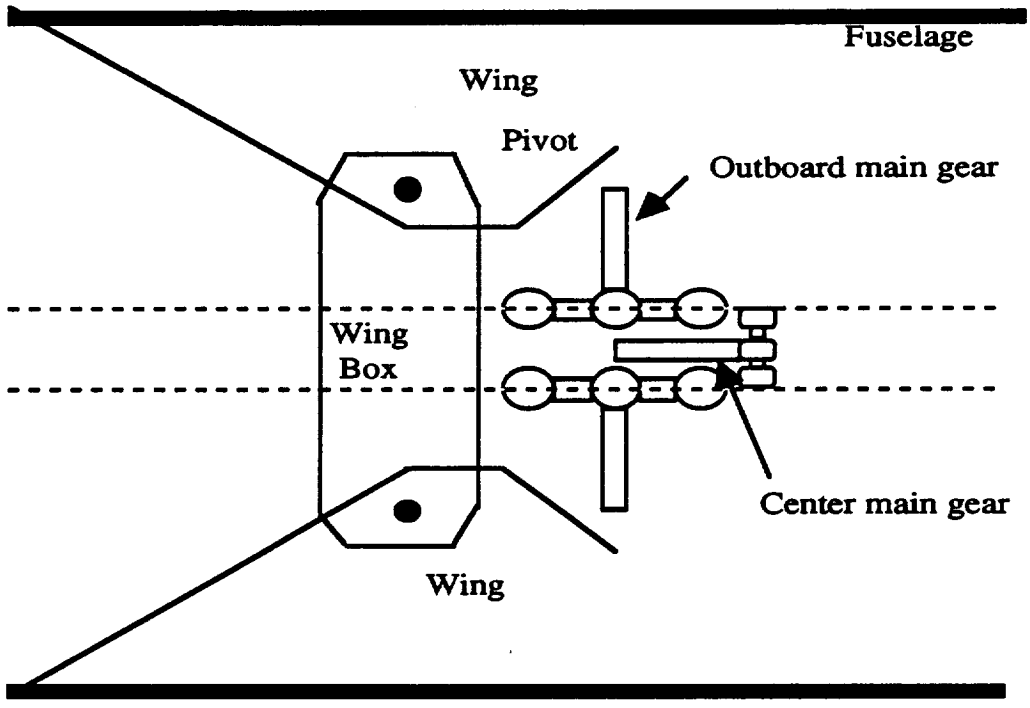

Figure 7.7 Landing gear retraction into the fuselage

The tires chosen were the same for all of the trucks. This will provided a maintenance benefit, as well as eliminate the stocking of different size tries for the main gear and the nose gear. Tire dimensions are presented in Table 14.

Table 14 Landing Gear Tires

Quantity	17
Dimensions	46" x 16"
Pressure	245 psi
Rated to	52000 lbf
Total load carrying capacity	884,000 lbf

The outboard main gear trucks retract inward while the center main gear truck retracts directly aft and the nose gear retract forward. This will allow the gear to free fall into the locked position in the event of a hydraulic failure that would normally prevent the gear from being lowered. The retraction of the main gear and the nose gear are shown in the Figures 7.8 and 7.9.

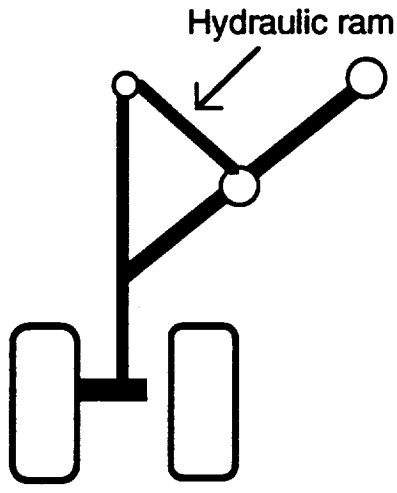

Figure 7.8 Retraction of the Main Gear
Front view

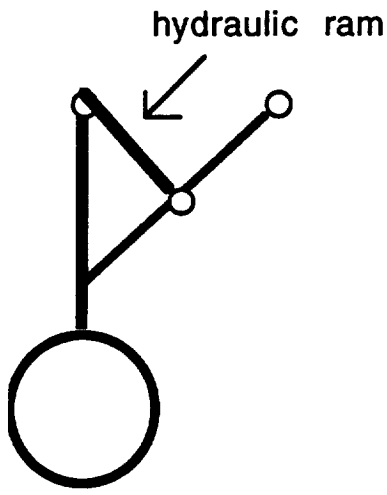

Figure 7.9 Retraction of Nose Gear
Side view

The outboard main gear was composed of one bogey of six wheel trucks. These were chosen after examination of Reference 18, which showed that the required rigidity and damping could be achieved in this configuration. This large number of tires was necessary to distribute load over a large area in order to prevent damage to runways and taxiways due to over stressing the concrete with excessive shear loading. The center main gear truck was composed of three tires aligned along a single axle Figure 7.10. This third strut-truck component was required in order to further distribute the weight of this enormous aircraft over a larger area. The third strut also adds a degree of redundancy to the aircraft. The two outboard gear would suffice in the event of a failure of the center strut to deploy. The nose gear is a standard two wheel truck arrangement as typical of the many commercial aircraft today Figure 7.11.

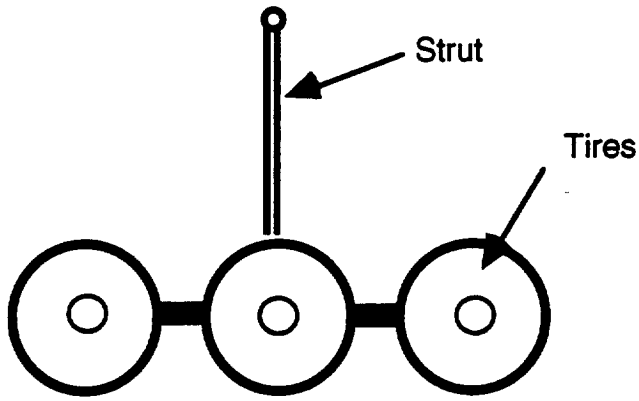

Figure 7.10 Main Gear Truck
Side view

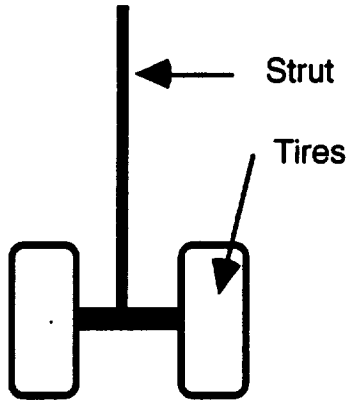

Figure 7.11 Nose Gear Truck
Front view

Another major concern of the landing gear configuration was the rotation angle allowed by the placement of the landing gear. Again the landing gear was a major factor in the selection of the TBD[3] design. The aircraft's rotation angle of ten degrees necessary for liftoff allowed a strut length that put the door sill height at 17.6 ft. (max. allowable for jet way) This configuration allowed the aircraft to be fully compatible with existing airport equipment.

8.0 STRUCTURES AND MATERIALS

8.1 Structures

TBD[3] V-n diagrams were constructed and it was found that TBD[3] was not gust critical at subsonic or supersonic cruise speeds. This simplified spar and wing box design because the gust loads did not have to be considered. Maximum positive n-force was set at 2.5 and maximum negative n-force at -1.0. These values are consistent with other transport aircraft and were recommended in Reference 2.

The subsonic case (Figure 8.1) was defined for Mach 0.85 cruise at 30,000 ft altitude and the supersonic case (Figure 8.2) was defined for Mach 3.0 at 60,000 ft altitude.(See Structures in Appendix). These conditions are those expected in overland and over water cruise respectively.

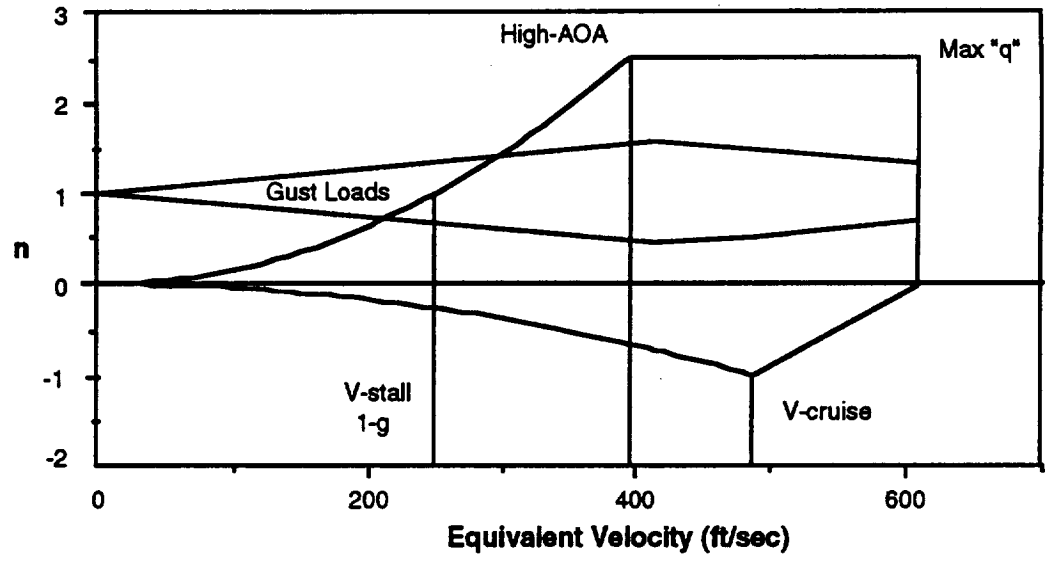

Figure 8.1 Subsonic V-n Diagram

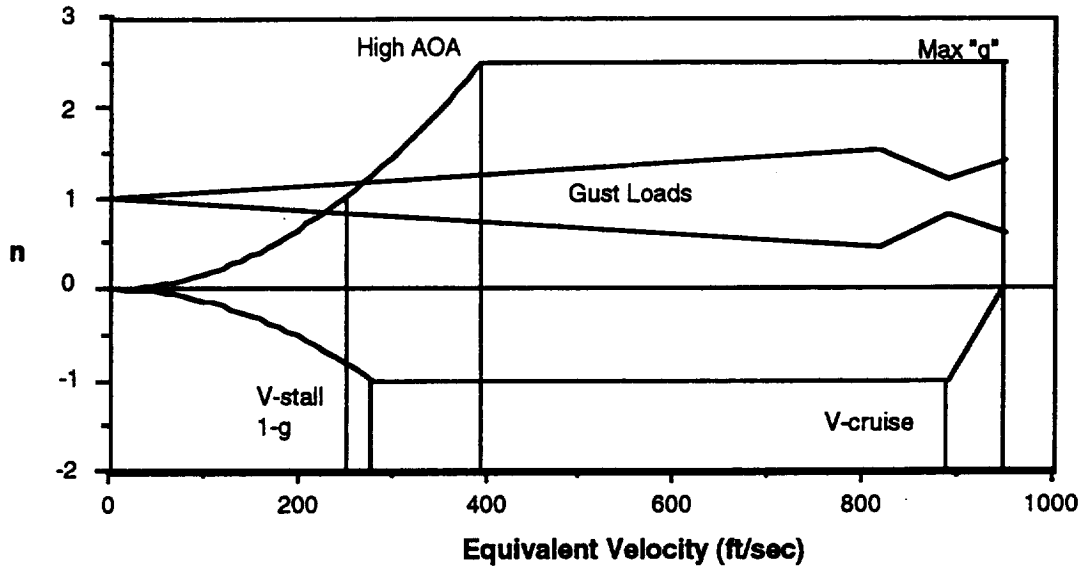

Figure 8.2 Supersonic V-n Diagram

The steps for the structural layout followed that of Reference 5. Special attention was paid to wing spar design, skin thickness, rib spacing, wing box design, frame spacing, and wing flutter.

Wing spar design was especially challenging. The TBD[3] had a 270 ft wingspan (subsonic) and a 4% thick, supersonic airfoil; both have adverse effects on wing structures and wing weight. The spar was intended to support aerodynamic loads and store fuel. The spar was designed to begin at half span of 33 ft. Inboard of 33 ft the fairing allowed for the thickening of the wing structure to join the wing box pivot mechanism (Figure 8.6). A design method was devised and programmed (see Structures in Appendix). The method multiplied the predicted spanwise lift distribution by the 2.5 load factor and a 1.25 safety factor and then subtracted the spanwise weight distribution to attain the effective force

distribution acting on the wing (Figure 8.3). Since the V-n diagrams showed that TBD^3 was not gust critical, the gust loads need not be included. The effective distribution was integrated two times to derive the spanwise moment distribution (Figure 8.4). Maximum allowable stress was limited to 100 ksi (narrowing material selection to titanium and medium modulus carbon composites) and the minimum second moment of area (moment of inertia) was solved for. Figure 8.5 illustrates the spanwise minimum moment of inertia distribution.

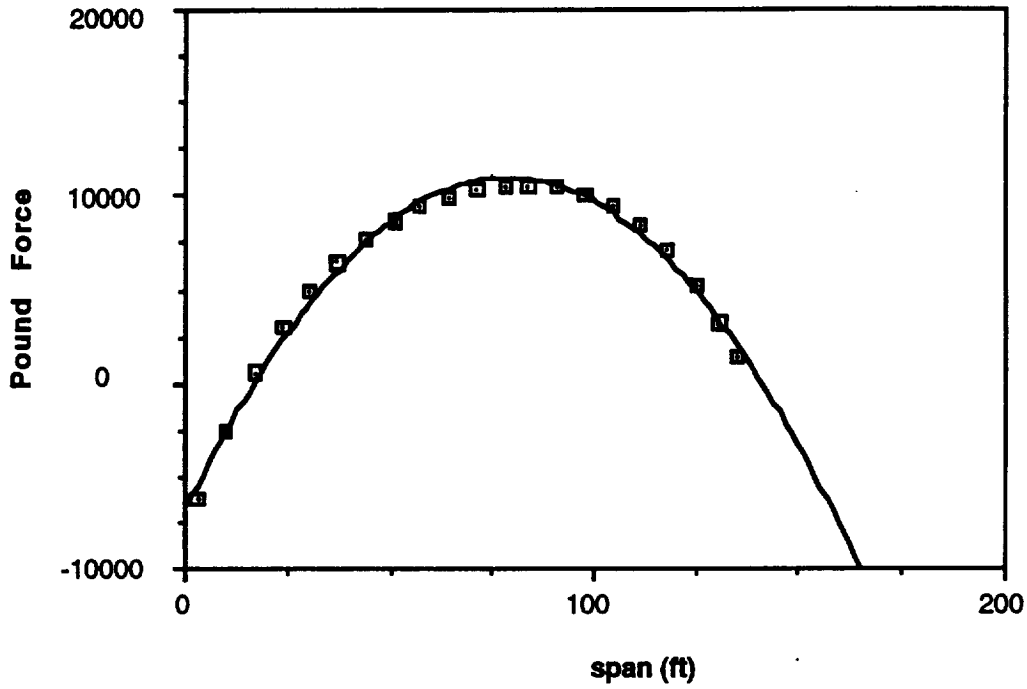

Figure 8.3 Effective Force Distribution

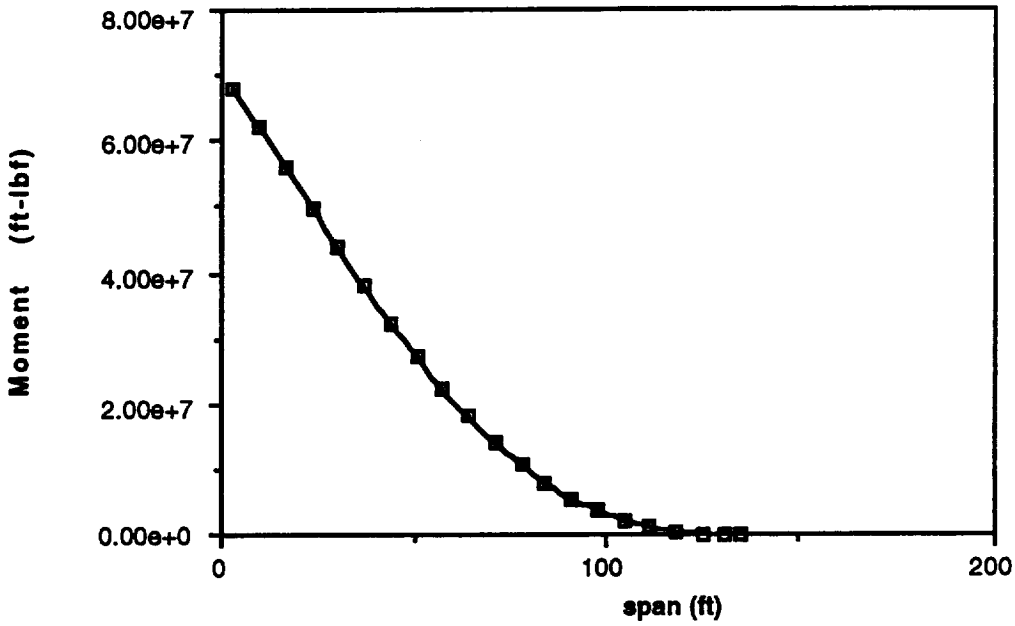

Figure 8.4 Moment Distribution

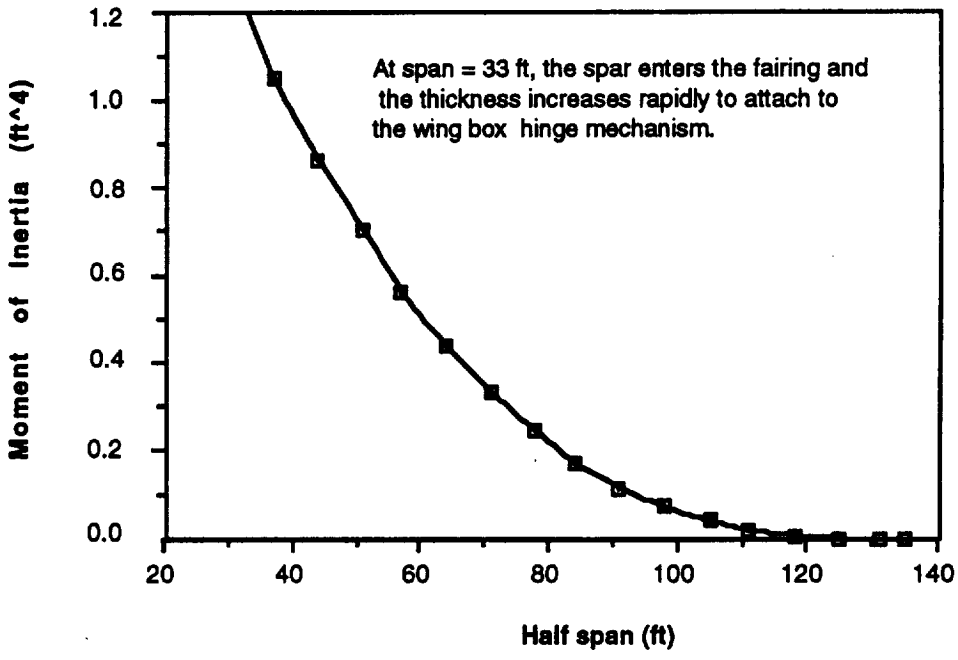

Figure 8.5 Minimum Allowable I

The spar was designed to have at least the minimum values in Figure 8.5 at all spanwise locations. It was not possible to attain the necessary moment of inertia with spar tubes alone while keeping weight and fuel volume values reasonable. The contribution of wing stringers to moment of inertia was accounted for. Finally, the available fuel volume in the wing was calculated and compared to the fuel weight in the original approximation of the weight distribution. If the weights did not agree reasonably well the process was iterated to a solution. Note that the analysis assumes a weight credit for the fuel contained in the spar during the initial force distribution estimation. This meant that the spar fuel cells must be full when the aircraft is at maximum take-off weight or failure could occur. At less than maximum take-off weight there would not be a problem. For example, if a wing fuel cell pump failed during flight, the aircraft would not be at max take-off weight, as the spar sizing analysis assumed, and there would be no danger.

The TBD[3] used a spar composed of as many six inch wide, bi-trapazoidal, carbon-fiber tubes as would fit between the leading and trailing edge control surfaces (Figure 8.6). The number and size of the tubes tapered with increasing span. The spar had constant area properties in five, twenty foot long sections. Each section was sized to meet the necessary moment of inertia of the inboard end and the geometry of the outboard end. This decision was based on producability considerations. The constant cross section lended itself nicely to pultrusion technology which does not allow for tapered tubes. This dramatic reduction in production complexity and cost was accomplished with a low weight penalty of only about 200 lbf per aircraft. This penalty was estimated by crediting the weight loss due to thinner necessary wall thickness of the tubes and crediting the added fuel weight in the wings. If it was determined that the

the added fuel weight in the wings. If it was determined that the weight savings were worth the added expense and complicated production technique of fitting each spar tube to the airfoil shape, the new spar could be easily implimented. Only the shape of the ribs would need to be redesigned. Table 15 presents geometry of each section and shows a representative cross section. T1 and t2 are the thickness of the horizontal and vertical sides of the spar tubes respectively.

Table 15 Wing Spar

Span (ft)	# Tubes	t1 (in)	t2 (in)	Section weight (lbf)	Fuel weight (lbf)
33-50	35	8/16	8/16	730	10699
50-70	32	7/16	7/16	577	9274
70-90	28	6/16	6/16	395	7489
90-110	24	5/16	5/16	265	5852
110-130	20	4/16	4/16	165	4377

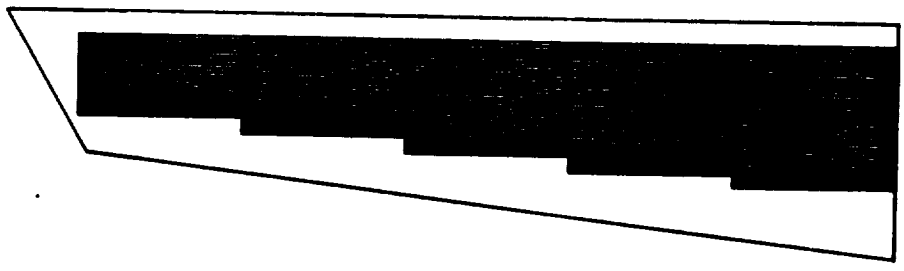

Figure 8.6 Wing Spar Top View

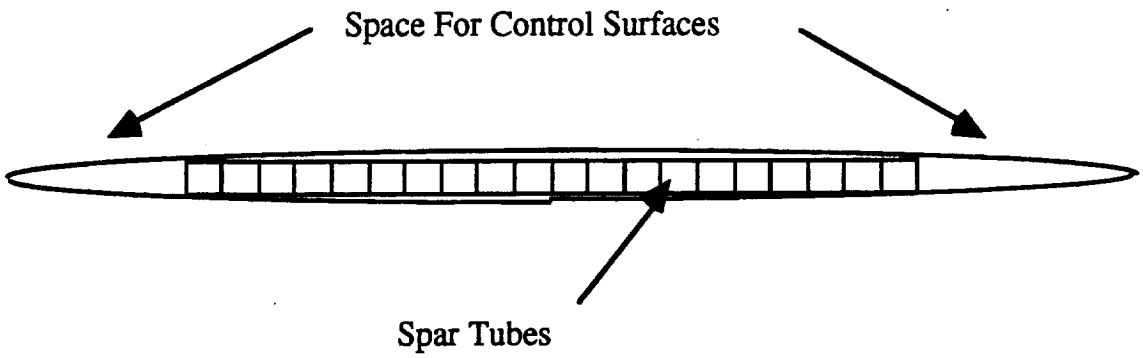

Figure 8.6 Continued Wing Spar Cross Section

The spar turned out to be orders of magnitude oversized for torsion. This was a very convenient coincidence because it ensured that TBD^3 would not experience aileron control reversal during cruise.

Wing rib shape can be inspected in Figure 8.6. Ribs were placed every 16 inches based primarily on historical data.

The wing box (Figure 8.7) design and pivot mechanism used on the B-1 bomber was resized of to carry the TBD^3 moment distribution integrated over the entire span. The torsion moment caused by the effective force distribution with the wings in cruise position (swept aft) was found to be greater than the pitching moment in any configuration. The pitching moment was therefore neglected in the wing box design. The wing box also had to be designed so landing gear could safely attach to it. Also, the fuselage was reinforced with extra frames and longerons within 20 ft forward and aft of the wing box to distribute torsional loads. It was intended for the 1700 ft^3 volume contained within the wing box to be used for fuel storage.

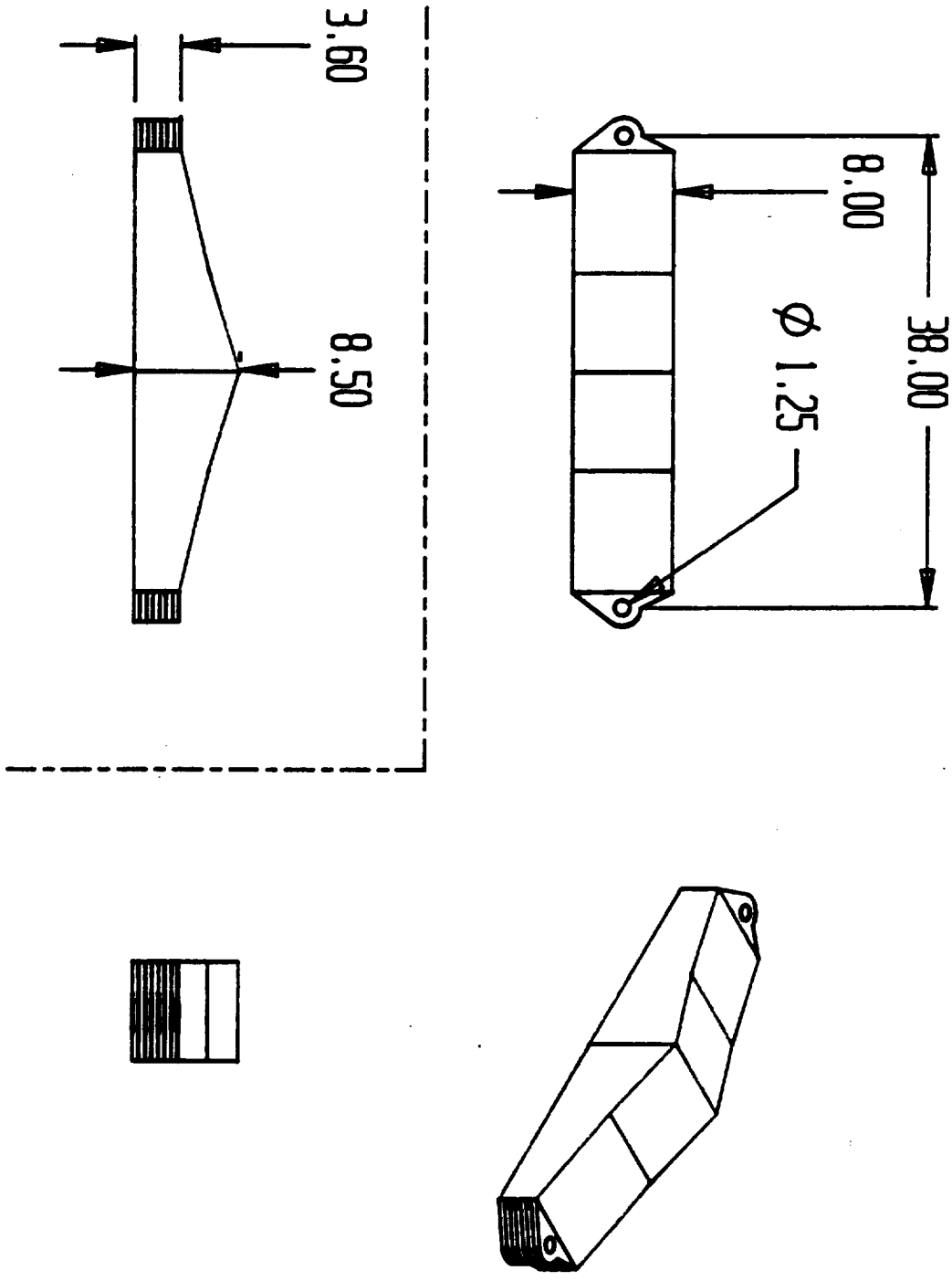

Figure 8.7 Wing Box

The fuselage was laid out similar to the instructions of Reference 3 Longerons were spaces 14 inches apart except within 20 feet of the wing box. At this high stress location, longeron spacing was decreased to 6 inches.

Fuselage frames were spaced slightly further apart than suggested by Reference 3, again with the exception of within 20 feet of the wing box. Typical frame spacing is 16-20 inches on other transports, but this spacing is largely determined by the need to have a frame between every window. Since the TBD^3 had no windows the frames were spaced at 24 inches. The spacing was decreased to 12 inches near the wing box for increased strength.

Skin thickness was sized by the stress in the skin due to the pressure differential at a 60,000 ft altitude. Cabin pressure was assumed 7,000 ft. An efficiency of 0.80 was assumed and the titanium skin needed to be at least 1/64 inch thick. This was increased to 1/32 on the nose to alleviate aerodynamic heating concerns and thickened to 1/32 inch within 20 feet of the wing box for increased strength.

A structural dynamic analysis of TBD^3 to determine critical speeds for wing flutter, wing divergence, and control reversal speeds was initially undertaken, but soon after abandoned. Independent research, as well as, professional consultation from structural dynamics professors, structural dynamic experts in industry, and structural dynamic experts in military flight test programs, suggested that any analysis done by TBD^3 designers would be an exercise in futility. This type of analysis is typically performed with the aid of NASTRAN, and years of flight test experience is then needed to "massage" the NASTRAN results. Even with a detailed structural and mass distribution model, massaged

NASTRAN results are not always fully trusted until actual flight test data is taken. The undertaking would be more suited to a doctoral dissertation than to a sub-section of an aircraft design report.

An alternate route to structural dynamic analysis was chosen. Professional consultation was sought from engineers at Rockwell International and flight test engineers at the Air Force Flight Test Center at Edwards AFB, Ca., who had experience with in B-1 flight test program. Dynamic pressure was said to be the most important parameter in quantifying flight test data. Figure 8.7 shows actual B-1 flight test data attained from Rockwell.

With a detailed second moment of area and mass distribution model (not available in preliminary design), this data could be appropriately scaled to predict TBD^3 behavior to within an order of magnitude. This data could not be scaled to fit aircraft with delta wings because they are not structurally similar to the B-1. Note in Figure 8.6 that data is taken at much lower altitudes and lower velocities than are intended for TBD^3 The data was still applicable; however, dynamic pressure, the critical parameter, is a function of velocity and density (altitude). TBD^3 flies much faster, but the density at 60,000 ft is only 0.09413 that of sea level, and dynamic pressure is comparable. Also note that the critical transonic-sonic flight regime is of highest concern. The critical values of dynamic pressure for flutter are high for subsonic and supersonic flight and these areas of TBD^3 flight regime are not forseen to be flutter prone.

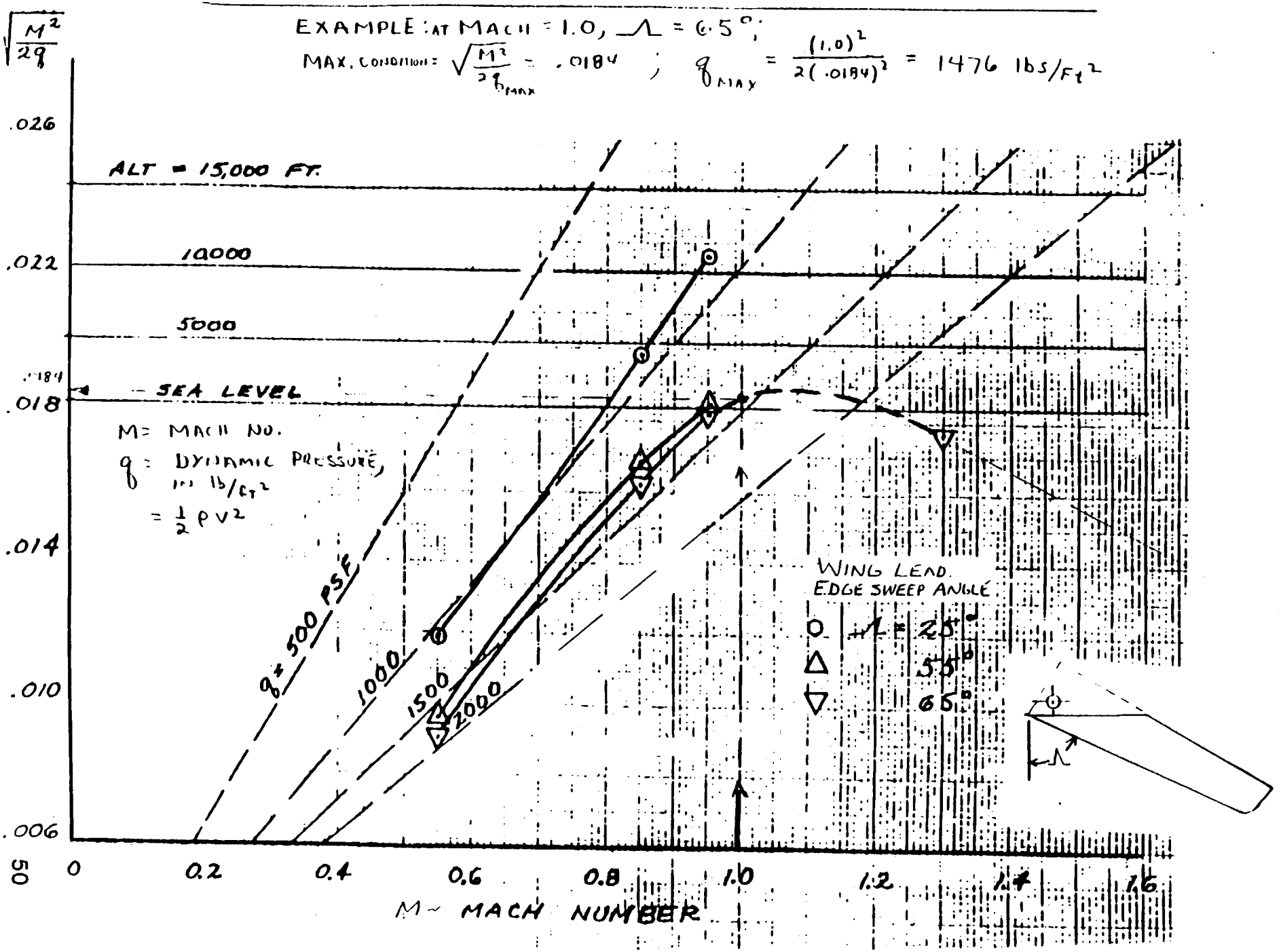

Figure 8.8 B-1 Flight Test Data

8.2 Materials

Materials were selected for both their structural and thermal properties. It was found in Reference 5 that average skin temperatures would be 430-450°F. Temperatures well above this were expected at stagnation areas such as the nose, wing leading edge, and tail surface leading edge. Conventional aluminum construction was not possible at these elevated temperatures. Aluminum was only used for internal structures such as frames, stringers, and ribs.

The TBD^3 wing spar also demanded exotic materials. Only a material with allowable combined thermal and cyclic stress of 100 ksi could be used. Without this high failure stress, the necessary wing spar tube thickness increased to unreasonable values. This led to a heavier spar because of the increase in material and the decrease in available fuel volume. Another item that was appropriately constructed of non-aluminum material was the wing box The box and swing mechanism carried an assumed weight penalty that led other designers to abandon the swing wing approach. With the age of improved composite manufacturing techniques approaching, composite primary structures were used on the TBD^3. When the weights of the composite wingspar and wing box were summed, the weight penalty was found to be only the hydraulic system used to swing the wings. Table 16 lists the major structures and materials.

Table 16 Material Selection

Item	Material	Primary Reasons
wing box	carbon composite	weight, strength
spar	carbon composite	weight, strength
all skins	titanium	thermal
L.E. heat sink	beryllium	thermal
frames, longerons	aluminum	cost, machinability
wing ribs	aluminum	cost, machinability
floors	fiber glass	weight, cost
landing gear	steel	strength, cost

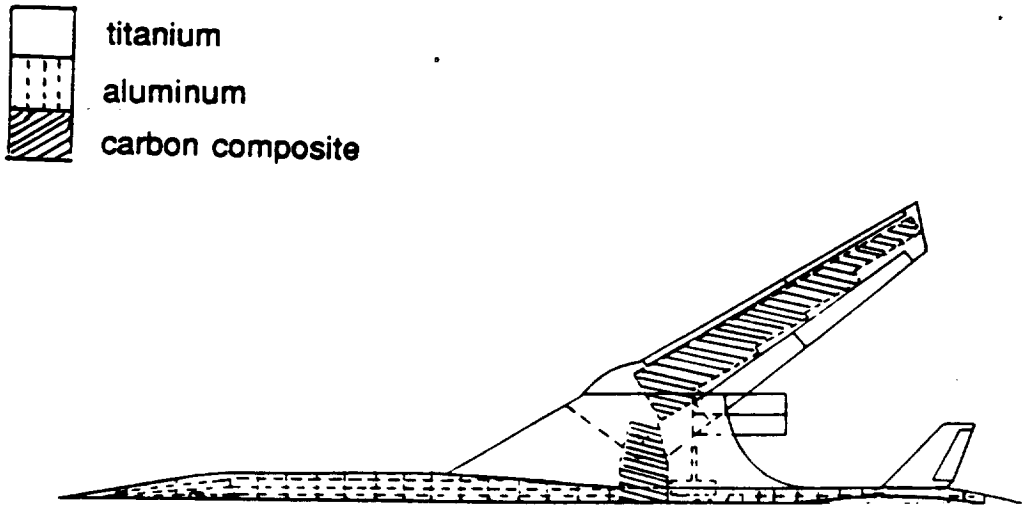

Figure 8.9 Materials Layout

Passenger and crew comfort was of utmost concern. A cooling system was designed to maintain 70°F in the passenger compartments. A Johns Manville insulation product called Min-K was found to perform well for TBD[3]. The cooling system consisted of a thin layer of Min-K 1301 adjacent to the titanium skin and a second, thicker layer of Min-K 501. Additionally, a refrigeration system was used to remove what heat transferred through the insulation as well as the heat generated by the passengers and crew. This layer of insulation was designed to cover the inside of the fuselage from the flight deck to the end of the first class passenger compartment. Table 17 presents the cooling system with associated weights.

Table 17 TBD[3] Cabin Cooling System

Item	Thickness (in)	Weight (lbf)
Min-K 1301	0.10	1010
Min-K 501	1.66	8390
Refrigeration System	NA	600
Total		**10,000**

9.0 AIRCRAFT MASS PROPERTIES

9.1 Weight and Balance

The method used to obtain the take-off and empty weights of the TBD^3 supersonic transport are outlined in References 1 and 2. In the preliminary design phase, the method presented in Reference 1 was employed to attain overall weights such as the weight of the fuel burned, OEW, and take-off gross weight. This method yielded the values presented below.

Table 18 Weights in Preliminary Design

Operating empty weight	350,000 lbs
Weight of fuel burned	400,000 lbs
Take-off gross weight	750,000 lbs

Examination of similarly sized aircraft showed that these were reasonable weights compared to historical data, but it was felt that the weights were too low for an aircraft with the flight specifications called for in the RFP.

At this point, TBD^3 was broken down into components and a sum of individual weights were obtained as outlined in Reference 2 (Section 9.2 of this report). This was a necessary step in order to achieve the aircraft center of gravity in the various configurations afforded by the variable geometry wing planform. Reference 2 presents an extensive list of parametric equations for estimating the weights of individual components. These equations were tested on an existing aircraft and were proven to be valid. The take-off gross weight

calculated by these equations were more accurate than the values obtained using the method above. This method yielded the values presented below.

Table 19 Weight of the TBD[3]

Operating empty weight	380,000 lbf
Fuel burned weight	400,000 lbf
Take-off gross weight	780,000 lbf

9.2 Component Weights and Location

Component weights were used in the center of gravity calculations (Table 20).

Table 20 Component Weights

Component	Weight (lbs)	Component	Weight (lbs)
Wing panels	94300	Seats, Fixtures	7500
Wing shoulders	40410	Fuel systems	4800
Fuel (panels)	210000	Instruments	2300
Fuel (shoulders)	187000	APU	1500
H-Tail	7500	Hydraulics	1800
V-Tail	9700	Pneumatics	1700
Fuselage	46000	AC power	2400
Nose gear	4300	DC power	350
Main gear	39000	Electrical lighting	1500
Passengers	45000	Air conditioning	4000
Engines	51500	Ice protection	500
Insulation	11000		

Simple geometric modeling was used to determine the geometric center of the components, and then the effect of any changes in density within the component due to structures was estimated. This procedure was used to locate the centroid of each component. Taking the nose as a reference point, the lateral center of gravity was calculated for various configurations and load scenarios. The systems were all placed to locate the c.g. for favorable

longitudinal stabilities in each configuration (See section 11.1). The result of these calculations can be seen in Figure 9.1 and 9.2 in the form of the center of gravity excursion plot.

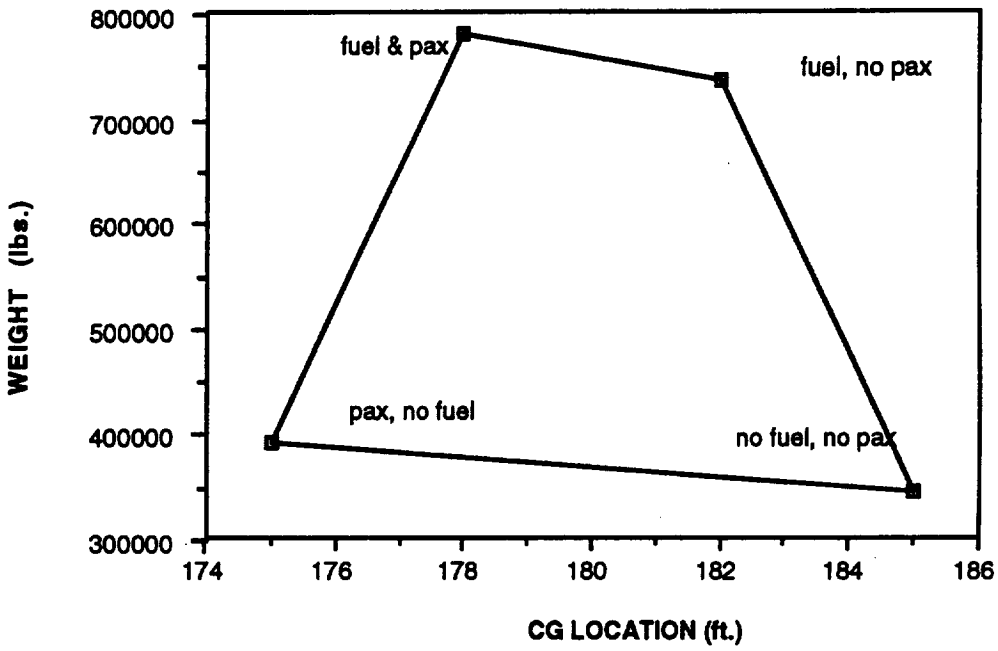

Figure 9.1 C.G. Excursion Plot, Wings Swept

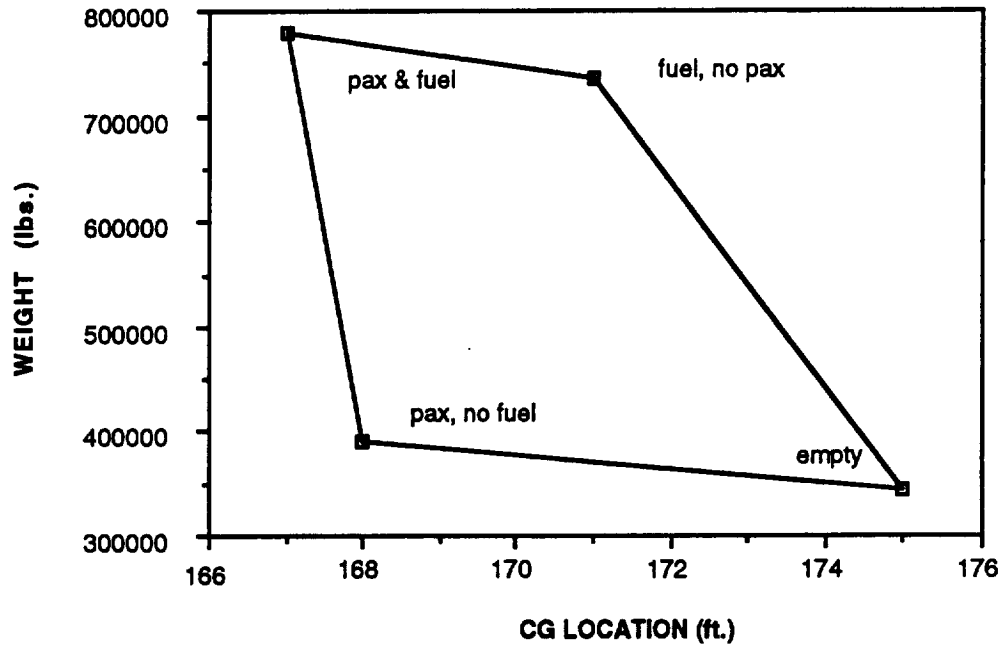

Figure 9.2 . Excursion Plot, Wings Forward

As shown, the total c.g. travel is about ten feet for each configuration. The resulting change in longitudinal stability was easily dealt by the fly by wire system. The c.g. shift with wing movement proved not to be a problem due to the a.c. shift that accompanied the wing movement (See Appendix).

10.0 AERODYNAMICS

10.1 Airfoil Selection

A four percent thick biconvex airfoil was selected for the TBD^3 (Figure 10.2). This was dictated by the mission requirements of the aircraft (See section 2.0). For a High Speed Civil Transport, a low drag coefficient at supersonic speeds was deemed crucial. This parameter dictated that the airfoil section needed a sharp leading edge, as the wave drag penalties for a blunt shape were too severe. A section with rounded upper and lower surfaces was chosen over more optimal supersonic sections, such as double wedge designs (Reference 22), because of the need for the aircraft to take off in populated areas at high gross take off weights. Sections with sharp corners on the surfaces showed problems maintaining attached flow at subsonic conditions. This limited the C_l's of such sections so severely that a fully loaded civil transport employing a double wedge design could not operate in and out of contemporary airports due to runway length and noise restrictions. The problem of maintaining attached flow still applied at the leading edge of the biconvex section. This problem was solved with the addition of a variable deflection leading edge as used on modern high performance air superiority aircraft. The deflection angle would be controlled by the flight control system and would orient the sharp edge into the incoming flow at all times. Analysis using panel methods such as PANDA showed that flow would remain attached to the upper surface if attachment could be achieved at the leading edge. This analysis as well as the existing use of such systems verified this approach as a solution to the problems associated with sharp leading edges.

Once the general shape of the airfoil was established, a thickness had to be selected. High thickness was desirable for reducing the weight of structures, while increasing the maximum lift coefficient and fuel storage volume. However, a thick wing section would severly increase wave drag (Reference 20). Once again, the importance of minimizing cruise drag restricted the thickness to 4 percent chord. Restricting the thickness to such a low value also increased the critical Mach number to 0.9. This allowed high cruise speed without the onset of severe wave drag penalty (Figure 10.1).

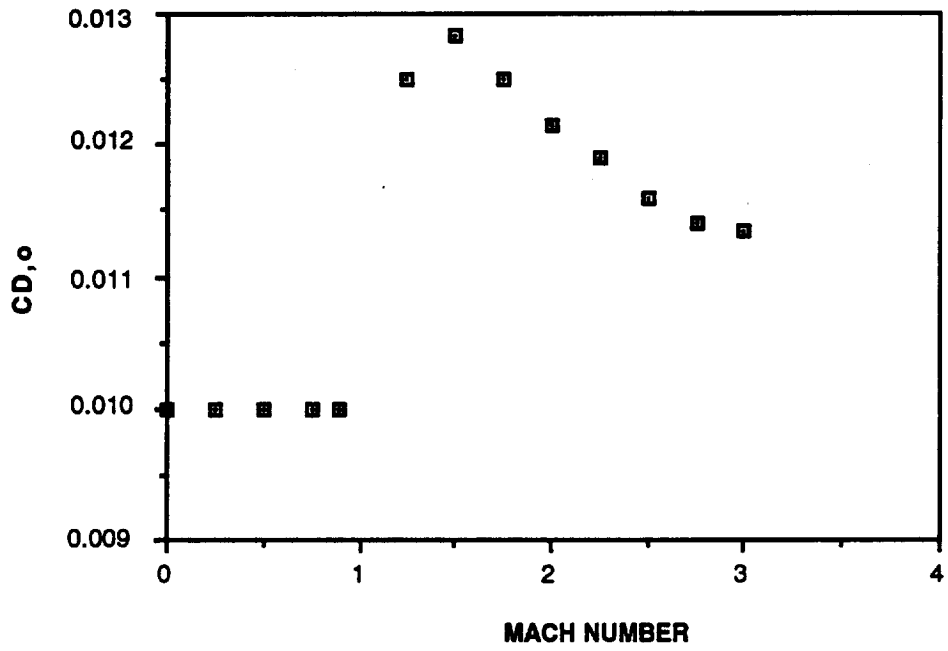

Figure 10.1 Profile Drag vs. Mach Number

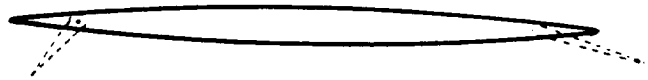

Figure 10.2 Four Percent Thick Biconvex Airfoil

The following characteristics applied to the airfoil selected:

Table 21 Wing Airfoil Characteristics

t/c	0.04
Point of maximum thickness	0.5 c
$C_{l,o}$	0 (for no L.E. deflection)
Lift curve slope	0.110 /deg. (subsonic)
Lift curve slope	.070/deg. (supersonic)
C_l max	1.2

NACA 0009 airfoils were chosen for both the horizontal and vertical tails. The need for good low speed performance without the complexity of leading edge devices outweighed the wave drag penalty due to the round leading edge for these surfaces. This proved to be the thinnest section that would generate high

enough C_l's without leading edge devices (Reference 9,19). The characteristics of the NACA 0009 are in Table 22.

Table 22 Empennage Airfoil Characteristics

t/c	0.09
Point of maximum thickness	0.35 c
$C_{l,o}$	0
Lift curve slope M<1	0.110 /deg
Lift curve slope M>1	.070/deg
C_l max	1.2

The NACA 0009 airfoil used on the empenage surfaces is pictured in Figure 10.3.

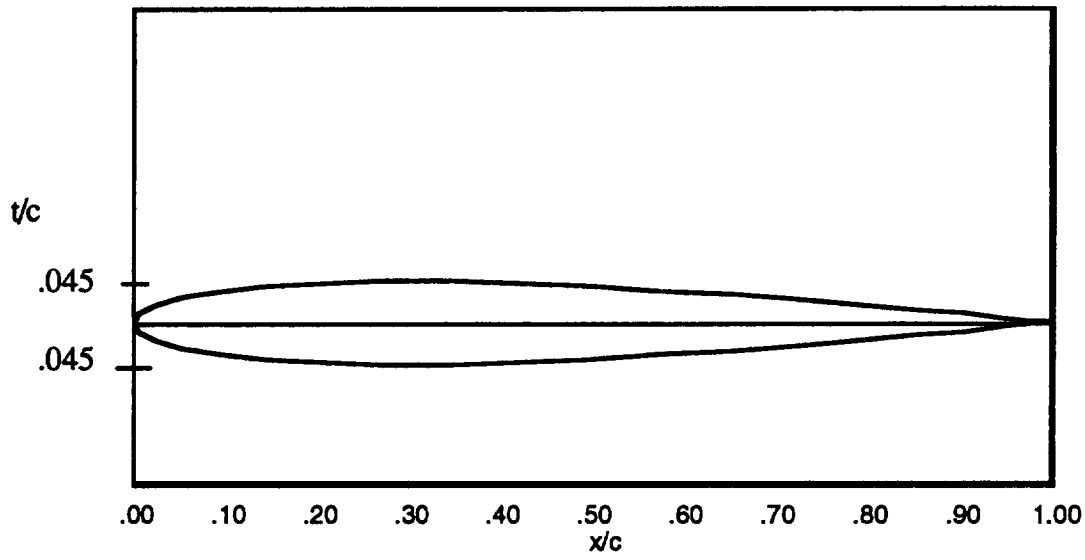

Figure 10.3 NACA 0009 Airfoil

10.2 Lift Prediction

The lift generated by the variable sweep wing was analyzed in the most forward and aft swept positions to obtain the extreme cases. Several methods were used to predict the lifting characteristics of the planform and compared to confirm sound results. A panel method program (LinAir Pro by Desktop Aeronautics), a modified lifting line program (Reference 21), and an empirical method (Reference 6) were used. With the wings in the forward swept position, the agreement between the methods was consistent and each was used interchangeably depending on the ease of application. When the wings were in the most aft setting, the agreement was not as good (about 20% variation, See Appendix), so an average value from all three methods was used to be conservative. The lift curves are shown in Figure 10.4. As shown, the forward swept configuration gives superb lifting characteristics. This facilitates take off and landing at low speeds, increasing safety and reducing noise. The lift calculations for supersonic flight were computed using the method in Reference7, and the lift curve for this condition is shown in Figure 10.4.

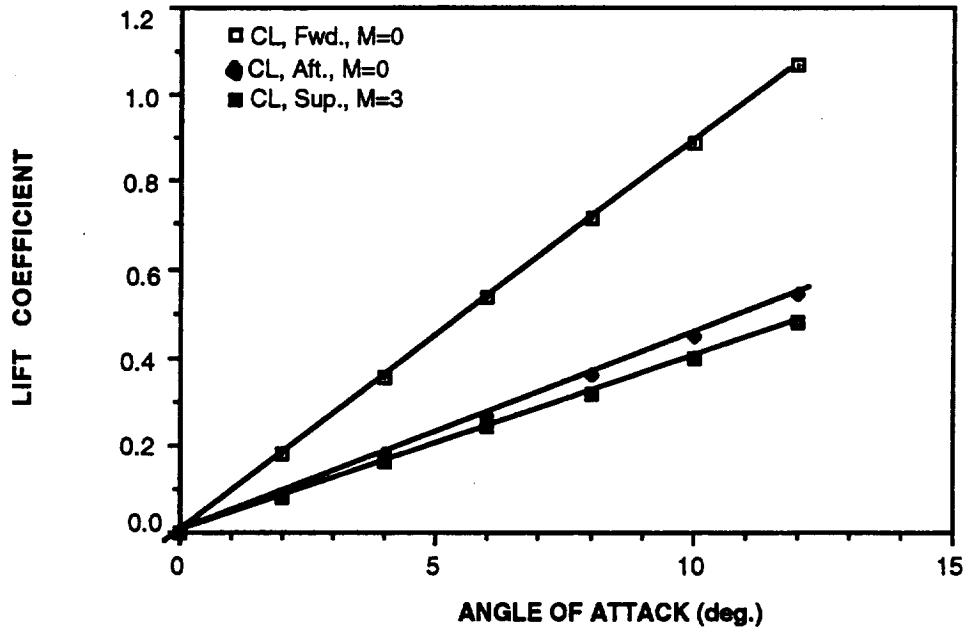

Figure 10.4 CL vs ALPHA

The maximum lift coefficients were found for different configurations using local lift coefficients derived from the above mentioned methods and maximum section C_l's. These are summarized in Table 23.

Table 23 Max Lift Coefficients

Wing Configuration	C_L
Wings Forward, Clean	1.2
Wings Aft, Clean	1.0
Wings Fwd., T/O Flaps	1.5
Wings Fwd., Landing Flaps	1.7

In the event of an emergency, the TBD^3 is able to land at maximum landing weight with the wings in the aft position and no high lift devices, offering a high level of passenger safety (see Appendix).

For the TBD^3 to take off from conventional airports, high lift devices must be employed. Fowler flaps were located along the inboard 35 percent of the semi-span, and flaperons were employed from sixty to eighty-five percent of the semi-span. These were sized using the method in Reference 2. Flaperons were used to increase the high lift capability without sacrificing controllability. For landing, the flaps and flaperons were deployed further than for take-off, hence the increase in $C_{L\ max}$. The leading edge of the main wing was equipped with a variable angle leading edge, thus keeping the flow attached on the surface of the airfoil. An added effect was the addition of camber to the otherwise symmetric wing section. This increased the effective angle of attack of the section by decreasing the zero lift angle of attack (Reference 19). This helped generate more lift at higher angle of attack where the leading edge was deflected most severely. No lift credit was taken for the leading edge device above that stated in Section 10.1.

10.3 Drag Prediction

The drag analysis was performed in four main parts: profile drag, induced drag, wave drag, and drag due to flap deflections.

To determine profile drag a computer program was written (see Appendix) that calculated wetted area, Reynolds number, and found the skin friction coefficient based on flat plate boundary layer theory (Reference 17). The program then added a form correction factor based on fineness ratio or thickness, and leading edge sweep. The program was validated using existing data for other commercial transports (see Appendix). Drag due to leaks and protuberances was added as three percent of the skin friction drag (Reference 2). Net interference drag was computed and found to be small and was left out of the final analysis for two reasons. First, the aircraft was reasonably well faired, which reduced interference between the wing and fuselage (Reference 2). Also, a study by Douglas Aircraft Co. (Reference 13) showed some powerful, constructive interference effects by placing the engine inlets just forward of the trailing edge of the wing. This study showed a net interference effect that increased L/D by up to 0.5 due to the external compression by the inlets. The inlets were placed in this position for this reason, and the positive interference was assumed to cancel the respective drag. The same program was used for the supersonic flight conditions, with two modifications. The skin friction equations were modified to reflect a compressible boundary layer, and the form factor was removed (Reference 2).

The induced drag was computed for subsonic and supersonic flight conditions, again using different methods for comparative purposes. For subsonic conditions, results from panel methods and lifting line theory were compared to obtain rigorous results for swept and unswept cases. For the supersonic case, induced drag consisted of the subsonic induced drag plus an additional drag due to lift known as wave drag. This is covered in the following section.

The wave drag calculations were performed in two parts: wave drag due to lift and wave drag due to volume. Wave drag due to lift was computed using a method suggested in Reference 2. This method is based on the lift curve slope found as indicated in Section 10.2. The Harris wave drag code, written by the Boeing Company, calculates wave drag due to volume with a numerical algorithm of Whitcomb's area rule given aircraft geometry. Unfortunately, the code was not available and a simpler method had to be found for wave drag calculation.

Wave drag due to volume was computed in two steps. A program was developed to calculate cross sectional area of an aircraft, perpendicular to the fuselage centerline (see Appendix), as a function of longitudinal coordinate. An approximation of a Sears-Haack body of revolution was attained through fuselage shaping. This shape was derived to minimize wave drag according to Whitcomb's area rule principal. The equation,

$$(D/q)_{WAVE} = E_{WD}\left[1-0.386(M-1.2)^{0.57}\left(1-\frac{\pi\Lambda_{LE^\circ}^{0.77}}{100}\right)\right](D/q)_{Sears-Haack}$$

where

$$(D/q)_{Sears-Haack} = \frac{9\pi}{2}\left(\frac{A_{max}}{L}\right)^2$$

was then used to calculate wave drag (Reference 2). Fuselage shaping and wave drag calculation were interdependent and iterated to the final solution. Figure 10.5 shows the TBD[3] equivalent body of revolution compared to a Sears-Haack distribution.

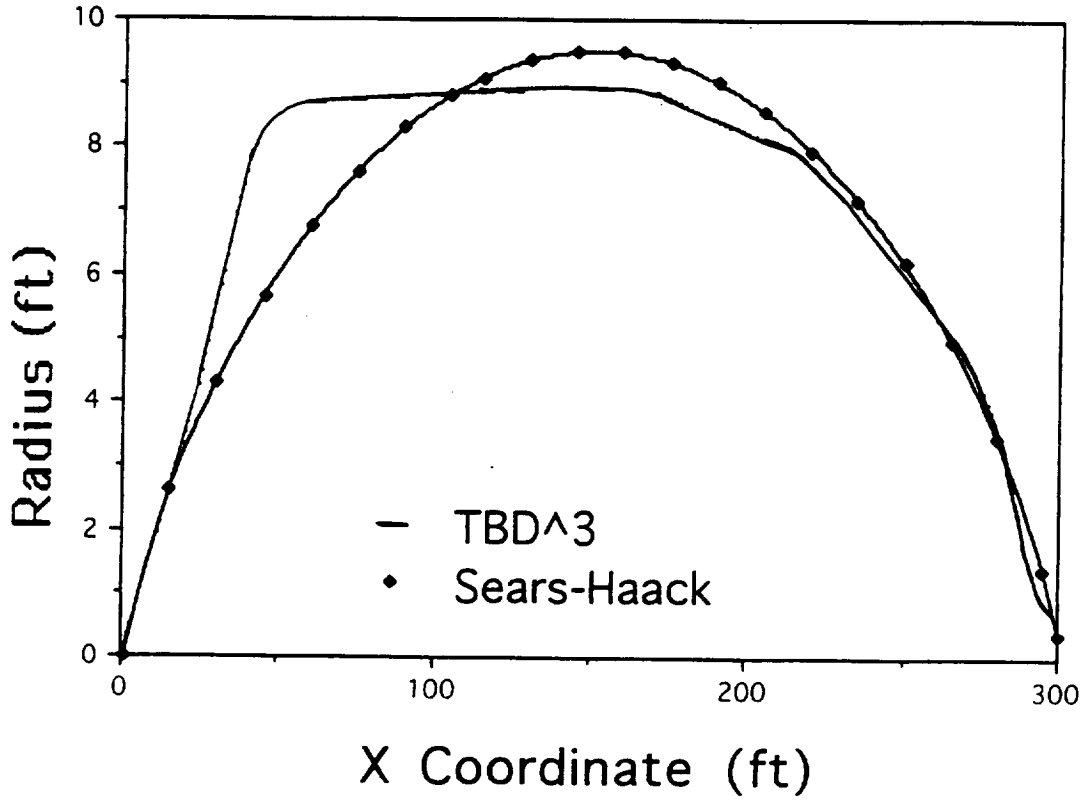

Figure 10.5 Equivalent Body of Revolution

The drag increment contributed by the use of high lift devices was also computed using the method in Reference 2. This was based on Fowler flaps over the inner span and flaperons outboard as mentioned in Section 10.2. Take

off and landing settings were individually computed so drag polars could be plotted for each configuration (Figure 10.6). No drag penalty was taken for the leading edge devices since no high lift gains were assumed.

The drag components determined in each of the analyses outlined above are listed in the following table. These values were used to construct the drag polars for several configurations as shown in Figures 10.6 and 10.7.

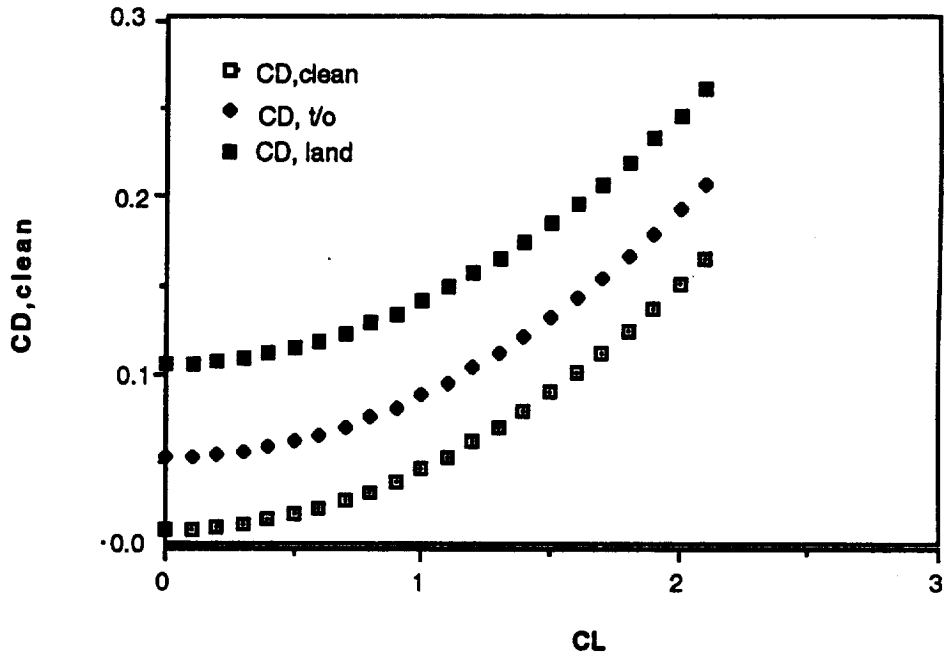

Figure 10.6 Drag Polar Wings Swept Forward
Take-off & Landing, Subsonic & Supersonic Cruise

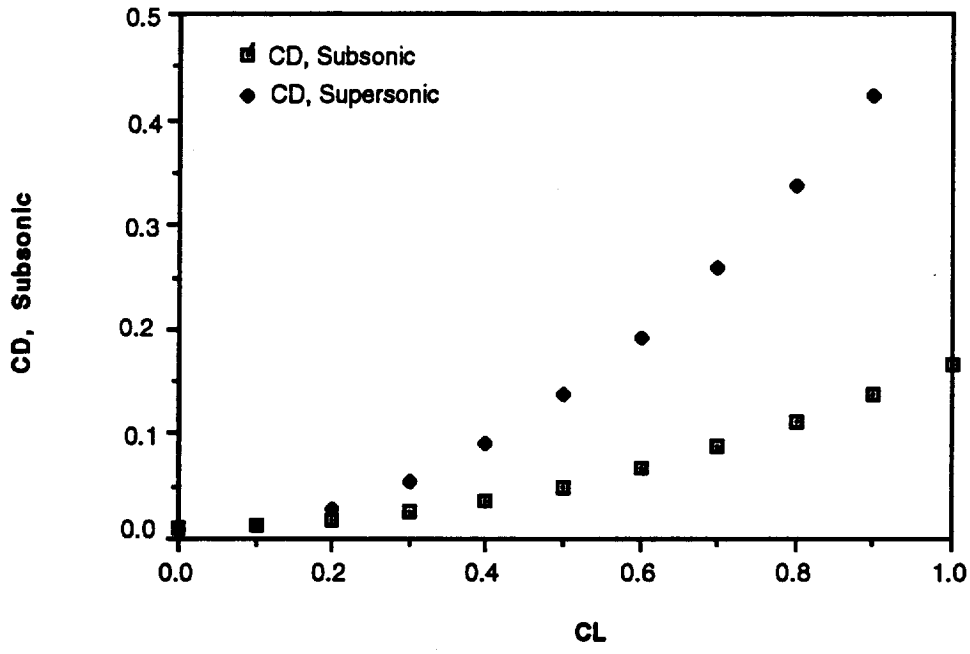

Figure 10.7 Drag Polar Wings Swept Aft
Subsonic and Supersonic Cruise

11.0 STABILITY AND CONTROL

The study of stability and control deals with primarily the action of the airplane to internally or externally generated disturbances. Since the design of the TBD^3 assumed an automatic control system, the main focus of the internal study considered changes in control surface deflections, changes in center of gravity location, and changes in the aircraft configuration (flaps, landing gear, variable sweep angles). The external study focused on the TBD^3's high altitude capabilities and temperature changes.

The TBD^3 was designed to be trimmable in all phases of flight. The variable geometry wing employed by the aircraft complicated this, but by strategic placement of fuel and systems the static margin was kept between plus and minus ten percent. This was only possible because the center of gravity and aerodynamic center both moved aft together as the wings moved into swept positions. The movement was found using the techniques of Reference 6 and the positions are illustrated in Figures 9.1, 9.2 and Table 24 (measured from aircraft's nose). The a.c. and c.g. remained close enough for the flight control system to maintain complete control of the aircraft (Reference 9). Rather than relying on control surface deflections to trim the aircraft, fuel pumping between tanks in different locations throughout the aircraft (Figure 12.1) was used to keep the center of gravity close to the aerodynamic center. This resulted in a near total elimination of trim drag in cruise configurations by eliminating the need for control surface deflections. Fuel pumping for trim was handled by the flight control computer reducing the workload of the pilot. This technique was added as a means of increasing aerodynamic performance and was not critical

to the safe operation of the aircraft. Should the fuel pumping system fail, TBD^3 remains trimmable in any configuration (c.g. location).

Table 24 Aerodynamic Center

Take-off & Landing	170 ft
Subsonic Cruise	180 ft
Supersonic Cruise	185 ft

The control surfaces of TBD^3 were initially sized using the method of volume coefficients outlined in Reference 3. These methods resulted in a geometry that enabled the calculation of the stability derivatives (see Appendix), from which was determined if sufficient control power existed (Reference 9). This process was iterated until all aspects of control power were at the required levels. The process gave the final empenage design outlined in Section 7.2 with the control surface sizes in Table 25. The static stability for this configuration are listed in Table 26.

Table 25 Control Surfaces

Control Surface	% span	% chord
Aileron	25	20
Rudder	80	40

Table 26 Stability Derivatives

	Take-off & Landing	Subsonic Cruise	Supersonic Cruise
$C_{y\beta}$	-0.564	-0.642	-0.533
$C_{y\delta R}$	0.131	0.148	0.103
$C_{y\delta_r}$	0	0	0
C_{yr}	0	0	0
C_{yp}	-.026	-.029	0.021
$C_{n\beta}$	0.225	0.332	0.275
$C_{n\delta r}$	-0.052	-.077	-.053
C_{nr}	-0.176	-0.203	-.117
$C_{l\beta}$	-0.130	-.077	-0.071
$C_{l\delta r}$	0.005	0.008	0.006
$C_{L\delta e}$	0.327	-0.747	0.348
C_{lu}	0	0	0
C_{lq}	-0.595	-0.075	-0.047
C_{Lq}	4.01	-6.46	-0.616
C_{lr}	0.302	0.090	0.281
$C_{L\alpha}$	5.11	4.89	2.00
$C_{m\alpha}$	12.7	0.022	0.003
$C_{m\delta e}$	-1.08	-0.747	-0.747
C_{mu}	0.071	0.13	-0.032
C_{mq}	-9.47	-4.38	-4.13
C_{mtu}	0	0	0
$C_{mt\alpha}$	0	0	0
C_{du}	0	0	0
C_{txu}	0	0	0
$C_{d\delta e}$	0	0	0

Dynamic stability was also investigated for TBD[3]. The damping ratios and frequencies were calculated for the phugoid, short period, and dutch roll modes using the methods in Reference 9 (see Appendix). These are shown, along with the Spiral Mode time to double, in Table 27 for three aircraft configurations. All levels of dynamic stability proved within the limits of the flight control system (Reference 9).

Table 27 Dynamic Stability Derivatives

Take off Landing				
	Phugoid	Short Period	Spiral	Dutch Roll
Frequency (rad/s)	.171	2.89	n/a	.739
Damping	.0133	.151	n/a	.223
Time to Double (s)	n/a	n/a	8.81	n/a

Subsonic Cruise				
Frequency (rad/s)	.054	4.58	n/a	2.20
Damping	.00700	.0872	n/a	.0494
Time to Double (s)	n/a	n/a	2.42	n/a

Supersonic Cruise				
Frequency (rad/s)	.0157	4.12	n/a	5.65
Damping	.0424	.0321	n/a	.0113
Time to Double (s)	n/a	n/a	8.81	n/a

12.0 SYSTEMS

12.1 System Description

The systems used in the TBD^3 were chosen to reduce maintenance time and cost and were adapted to various flight operations. Since there aren't any windows in the flight deck synthetic vision will be used by the flight crew. Other systems used in the TBD^3 are:

-Electrical power
-Environmental control systems; used for air supply system, temperature control, pressurization control, and equipment cooling
-Electronic engine control and power; management control for engines
-Auxiliary power unit (APU)
-Flight controls
-Hydraulic system; swing wing hydraulic rams
-Landing gear retraction rams
-Landing gear auto-brakes, brake wear indication, and brake temperature monitor
-Communication; VHF, HF
-Audio; passenger service, entertainment, and passenger address
-Navigation; global positioning signal
-Lighting
-Antennas
-Ice protection for subsonic operation
-Fuel management system to control cg location throughout all flight regimes
-System pressure indication, fluid depletion detection, overheat detection, and other components as deemed necessary.

The hydraulic system used on TBD^3 will include the mechanism used for the swing wings. It also includes all the typical systems used on a conventional subsonic aircraft that manage the flight control systems. Fuel management system includes fuel pumps which will pump the fuel to various locations of the aircraft to control the c.g. location throughout flights. The navigation system used by TBD^3 is a global positioning signal which uses signal transmitted to the aircraft's system via satellite.

Environmental control systems are used for air supply system, temperature control of the cabin and equipment cooling. The cooling of equipment is achieved by the same systems used in subsonic aircraft. Since this aircraft will be built in year 2005, it is acceptable to assume a more sensitive cooling system will be developed. The cabin temperature is controlled by the fuselage insulation and refrigeration unit (See section 8.2).

12.2 System Layout

An illustration of the system layout is shown in Figure 12.1.

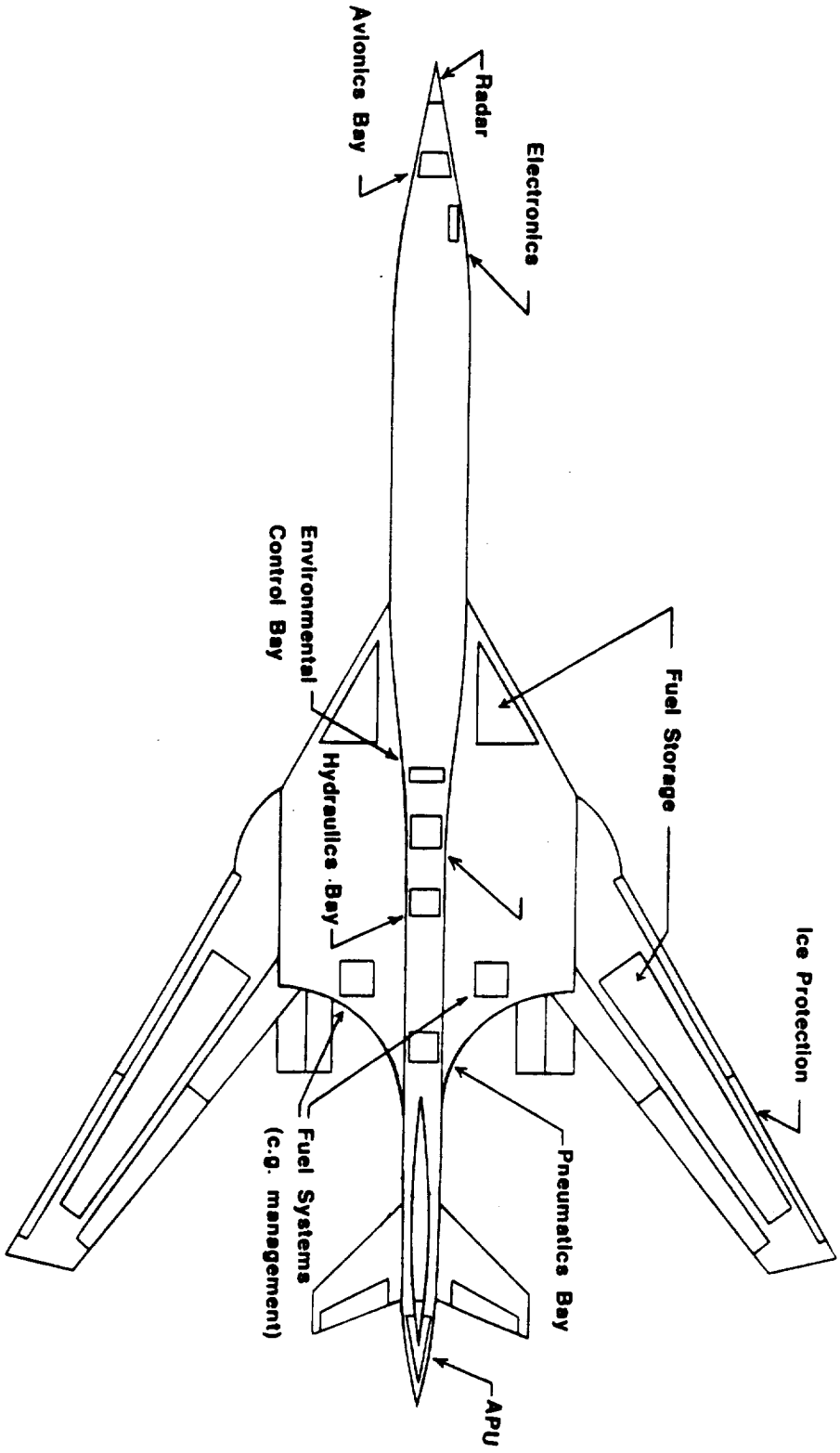

Figure 12.1 System Layout

13.0 MAINTENANCE REQUIREMENTS

The TBD^3 supersonic transport reparability and accessibility was compatible to the current civil transports in major airports. Simultaneous services were essential for TBD^3 to reduce ground time. These services included:

-Loading and unloading of passengers
-Loading and unloading of cargo
-Refueling and reoiling services
-Replenishing water supply
-Cleaning airplane cabin
-Removing and replacing food and beverages
-Servicing lavatories

Maintenance of the TBD^3's engines can be achieved by removal and installation of the engines separately by the maintenance crew. The overhaul work can be performed in existing hangars for large subsonic aircraft with only minor adaptations.

Since the materials used on the TBD^3 are expensive, new repair methods will be developed in order to allow structure repairs after damage instead of replacements of large structural parts.

An illustration of these simultaneous services is shown in Figure 13.1.

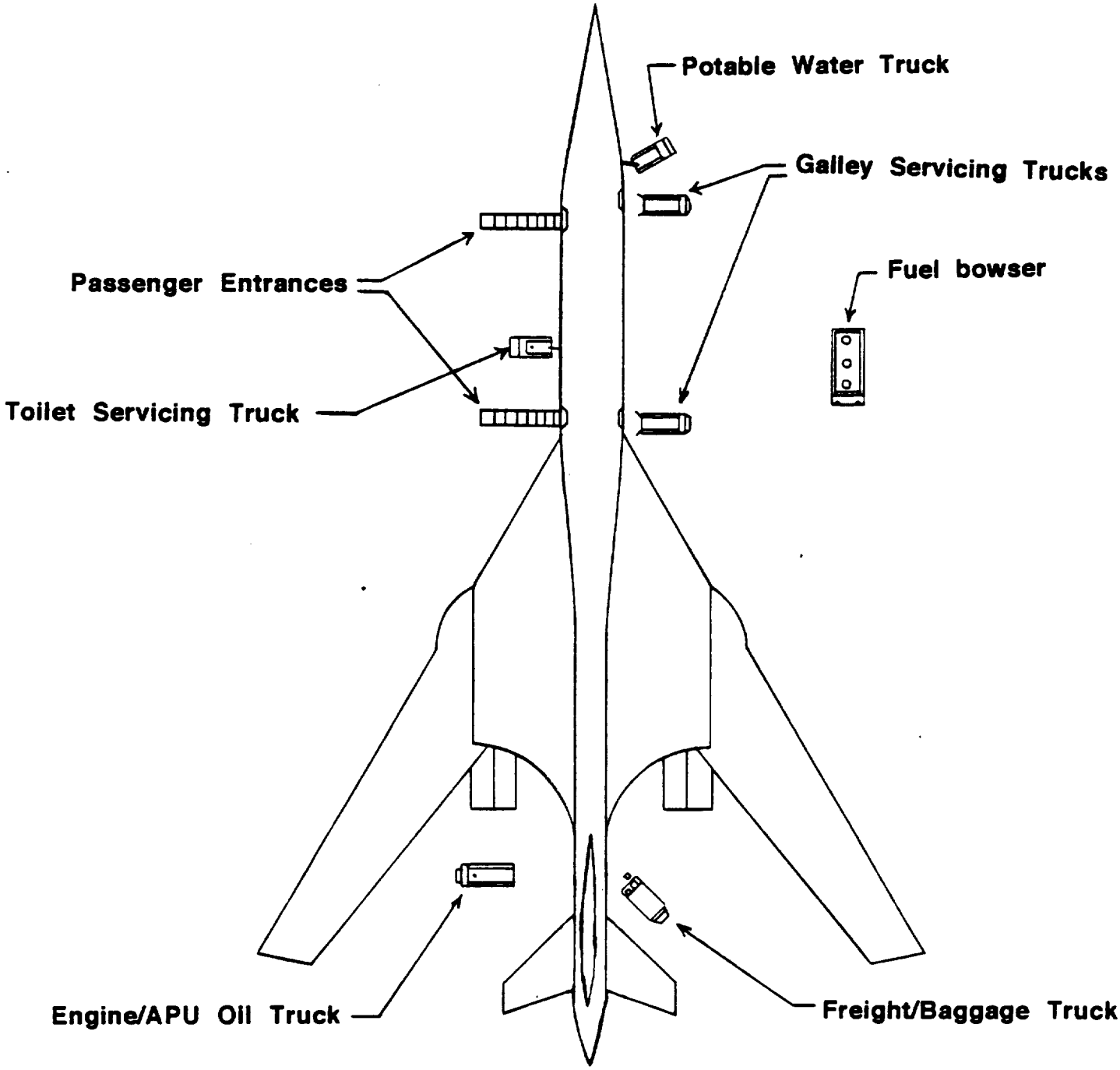

Figure 13.1 Aircraft Maintenance

14.0 COST ANALYSIS

Aircraft cost analysis was a delicate balance between science, art, and politics. Some of the cost estimation was based on prior aircraft cost, but since TBD^3 was a supersonic transport most of the cost estimations were a preliminary. At the end of this section a table presents the costs of the TBD^3 supersonic transport (Table 29).

TBD^3's cost was estimated using a combination of methods presented in Reference 1 and 2, and 14. Note that the cost of TBD^3 is based on 1992 dollars. TBD^3's cost was closely dependent on production quantity. The larger the fleet of aircraft the less expensive the aircraft could be produced. The purchase price of the TBD^3 was set to cover the research, development, test, and evaluation cost (RTD&E), and the interest paid by the airline to a bank. The interest rate used was the prime rate on loans. The profit for the airline was based on the cost of the aircraft (it has been assumed that the airline will require the aircraft to be paid off in 10 years) plus the direct and indirect operating cost to the airline minus the revenue which included the ticket sales for the airline and a salvage value for the aircraft after an estimated 15 years. The maximum limit on the ticket prices for an airline was set to be 20 percent above already existing first class rates for a similar range flight.

14.1 RDT&E and Production Costs

RDT&E and production costs were combined in the cost analysis of the TBD3. It included the engineering, tooling, manufacturing, quality control hours and development support, flight test, manufacturing materials. Engine production costs were also included, and the cost of avionics were estimated to be 10 million dollars per aircraft (Reference 14). The materials used in manufacturing was 10 percent composites, 30 percent aluminum, and 60 percent titanium (See section 8.2 of this report). A 12 percent interest rate had been added to the overall cost. This represented the total cost of the aircraft to the airline including the interest charged to the airline by the bank.

14.2 Operation and Maintenance Costs

Operation and maintenance costs included the fuel and oil cost, crew salaries, maintenance expenses, depreciation, and insurance costs. The current fuel cost of $0.90 per gallon had been used for the fuel cost estimation. The oil costs averaged less than half a percent of the fuel costs, and were ignored. Crew salaries included a two person flight crew and seven flight attendants. For maintenance expenses, material cost per man hour, and per maintenance cycle were present. It also included the maintenance man hour cost which has been estimated as $15.00 per hour. Depreciation of the aircraft and its engines were estimated using equations presented in Reference 2. The insurance paid by the airline was divided into two sections. Hull insurance which was 2 percent of the airframe cost, and passenger insurance which was $0.04 per passenger per nautical mile (Reference 14).

14.3 Direct and Indirect Operating Cost (DOC &IOC)

The operating cost of an airline was divided into direct and indirect operating costs. The direct operating cost was fuel, oil, crew, maintenance, depreciation, and insurance and was expressed as cost per seat-mile flown. TBD^3's DOC had to compete with future long-range wide-body civil transports to be economically feasible. TBD^3's supersonic capability allowed the airline to utilize the aircraft for more flights, therefore producing more revenue. Even though the direct operating cost of TBD^3 was higher than other civil transports, it was considered economically feasible.

The indirect operating cost of an airline included the advertising cost, ground crew salaries, management and other factors that vary with each airline. IOC was independent of the aircraft design and a reliable IOC analysis could only be done by the airline. However, in the request for proposal it was required that TBD^3 be compatible with existing airports and other facilities. The IOC used was assumed to be equal to the IOC for an existing subsonic long-range wide-body civil transport.

14.4 Airline Revenue and Profit

The revenue of the airline was primarily ticket sales. A load factor of 70 percent was assumed for the TBD[3] as an average load factor for airlines during a year. As previously mentioned the upper limit of the ticket prices is 20 percent above the existing first class rates (Reference RFP in Appendix). The ticket prices for a maximum range flight are shown in the table below.

Table 28 Ticket Prices

Class	Ticket Price
First	$4400.00
Business	$3850.00
Coach	$2200.00

The profit per year of the airline purchasing a fleet of supersonic transports was calculated by subtracting the sum of DOC, IOC, RDT&E, and production costs per year from the ticket sales per year considering a 70% load factor. The profit per year also included a 15 percent rate of return to the airline. The aircraft will be in operation for an average of 15 years, therefore a net profit of 15 years for the airline can be found by adding the salvage value of the aircraft to the profit. Note that the profit per year will decrease as the value of dollar decreases an average of 3% per year. This was taken into account when the net profit for the airline was calculated shown in table below.

Table 29 Cost Analysis of TBD[3]

RDT&E and Production cost/aircraft	$ 301,000,000.00
Fuel and oil cost/aircraft/year	$ 49,000,000.00
Crew salaries/aircraft/year	$ 969,000.00
Maintenance expenses/aircraft/year	$ 802,000.00
Depreciation/aircraft/year	$ 24,200,000.00
Insurance/aircraft/year	$ 6,060,000.00
DOC/pax/mile	$ 0.07
IOC/pax/mile	$ 0.03
Rate of return	15%
Airline profit per year/aircraft	$533,000,000.00
Salvage value	$30,100,000.00
Profit in 15 years	$6,310,000,000.00
Total profit in 15 years including salvage value	$6,340,000,000.00
Cost per aircraft (fteet of 300)	$301,000,000

C-2

15.0 CONCLUSION

TBD^3 met all design parameters that were set forth as goals in the revised version of the RFP. After many design trade-offs in the fuselage configuration, wing design, and engine types TBD^3 iterated to a realistic design solution to the challenges of a high speed civil transport. It is believed that the TBD^3 design outlined in this report would readily satisfy the future requirements of the second generation of supersonic transports. The design offers Mach 3.0 performance based on sound and usually conservative engineering, and proved to be economically advantageous.

Previously considered variable geometry designs have lost support because of the weight penalty commonly associated with a swing mechanism. The material science community is taking great and rapid strides towards the effective use of advanced composite materials and advanced metal alloys in aircraft manufacture. The weight penalty of incorporating a swing wing in the year 2005 was not foreseen to be an insurmountable challenge.

TBD^3 proved that the aerodynamic advantages more than compensated for the weight penalty. The most immediate advantage TBD^3 has over other designs is the ability to take-off and land efficiently and quietly. With the world's current public and legislative attitude toward environmental concerns the quiet take-off and landing capability alone will make the TBD^3 a fierce competitor in the civil transport market. Coupled with Mach 3.0 performance, TBD^3 promises to control a large share of the civil aviation business.

REFERENCES

(1) Roskam J., Airplane Design: Part I: Preliminary Sizing of Airplanes., Roskam Aviation and Engineering Corporation Rt 4, box 274, Ottawa Kansas, 66067

(2) Raymer D., Aircraft Design: A Conceptual Approach., p. 290, American Institute of Aeronautics and Astronautics, Inc. 370 L'Enfant Promenade, S.W., Washington, D.C. 20024

(3) Roskam J., Airplane Design: Part III: Layout Design of Cockpit, Fuselage, Wing, and Empennage: Cutaways and Inboard Profiles., Roskam Aviation and Engineering Corporation Rt 4, box 274, Ottawa Kansas, 66067

(4) Spotts Machine Design

(5) Corning G., Supersonic and Subsonic Airplane Design. Edwards Brothers Inc., Ann Arbor, Michigan. 1953.

(6) Roskam J., Airplane Flight Dynamics and Automatic Flight Control: Part I., Roskam Aviation and Engineering Corporation Rt 4, box 274, Ottawa Kansas, 66067

(7) USAF DATCOM

(8) Roskam J., Airplane Design: Part VI:.Preliminary Calculation of Aerodynamic, Thrust, and Power Characteristics, Roskam Aviation and Engineering Corporation Rt 4, box 274, Ottawa Kansas, 66067

(9) Roskam J., Airplane Design: Part VII:.Determination of Stability, Control and Performance Chacteristics: FAR and Military Requirements, Roskam Aviation and Engineering Corporation Rt 4, box 274, Ottawa Kansas, 66067

(10) Roensch R.,Fitzsimmons R., Advanced Supersonic Transport, Sociey of Automotive Engineers. Air Transportaion meeting. Hartford. Conn. May 6-8 1975.

(11) Fitszimmons R.,.Rowe W.T., Advanced Supersonic Transport. Propulsion Comparisons. Society of Automotive Engineers. Air Transportation meeting. Hartford. Conn. May 6-8 1975.

(12) Benson J.L., Sedgewick T.A.. AIAA/SAE 12th Propulsion Conference. AIAA Paper #76-756. July 26-29 1976.

(13) McDonnell Douglas Aircraft Company Study on Constructive Inteference. Presentation to the Aeronautical Engineerins Students. Feburary 1992.

(14) Economics data provided by McDonnell Douglas Aircraft Company. October 1991.

(15) Wiggins J.H. Jr., Effects of Sonic Booms, Published by Author, 1969.

(16) Niedzwiecki A., Ribner H.S., Subjective Loudness of Minimized Sonic Boom Waveforms. The Journal of the Acoustical Society of America. V64, pp.1622-1625, 1978.

(17) Anderson J., Fundementals of Aerodynamics. McGraw Hill. 1984.

(18) Boeing Aircraft Company's study on Landing Gear

(19) Abbot I., Van Doenhoff A., Theory of Wing Sections. Dover. New York. 1949.

(20) Bertin J. Smith M., Aerodynamics for Engineers. Prentice Hall. New Jersey. Second Edition. 1989.

(21) Ashley H., Landahl M. Aerodynamics of Wings and Bodies. Dover. New York. 1965.